








Adding value to aluminosilicate solid wastes to produce adsorbents, catalysts and filtration membranes for water and wastewater treatment

Daniela Gier Della Rocca¹ , Rosane Marina Peralta² , Rosely Aparecida Peralta³ , Enrique Rodríguez-Castellón⁴ , and Regina de Fatima Peralta Muniz Moreira^{1,*} 

¹Department of Chemical and Food Engineering, Federal University of Santa Catarina, Florianópolis, Brazil

²Department of Biochemistry, State University of Maringá, Maringá, Brazil

³Department of Chemistry, Federal University of Santa Catarina, Florianópolis, Brazil

⁴Department of Inorganic Chemistry, Crystallography and Mineralogy, University of Málaga, Málaga, Spain

Received: 17 July 2020

Accepted: 23 August 2020

Published online:

17 September 2020

© Springer Science+Business Media, LLC, part of Springer Nature 2020

ABSTRACT

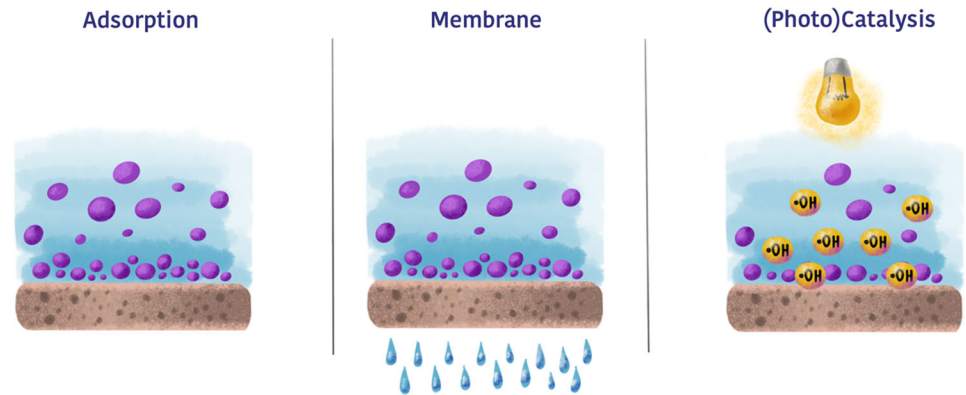
Geopolymers are a class of inorganic polymers that have attracted attention in recent years, especially in the construction sector, due to their promising mechanical properties, as well as simple and low-cost fabrication. These materials also stand out for being more environmentally friendly, not only because of their lower CO₂ emissions during production, but also because industrial by-products can be incorporated in their synthesis. Recent studies have investigated porous geopolymers, allowing expansion of their potential use to several other applications. Meanwhile, application of GPs to efficient water and wastewater treatments, such as nanofiltration and advanced oxidation processes, remains a challenge, especially due to high operational costs. Thus, this paper provides a comprehensive review of the current state of knowledge of geopolymers produced from aluminosilicate wastes, showing the main promising advances in their applications in three technological fields: (1) adsorption, (2) membrane filtration and (3) catalysis (as both catalyst or catalyst support).

Handling Editor: M. Grant Norton.

Address correspondence to E-mail: regina.moreira@ufsc.br

<https://doi.org/10.1007/s10853-020-05276-0>

GRAPHIC ABSTRACT



Abbreviations

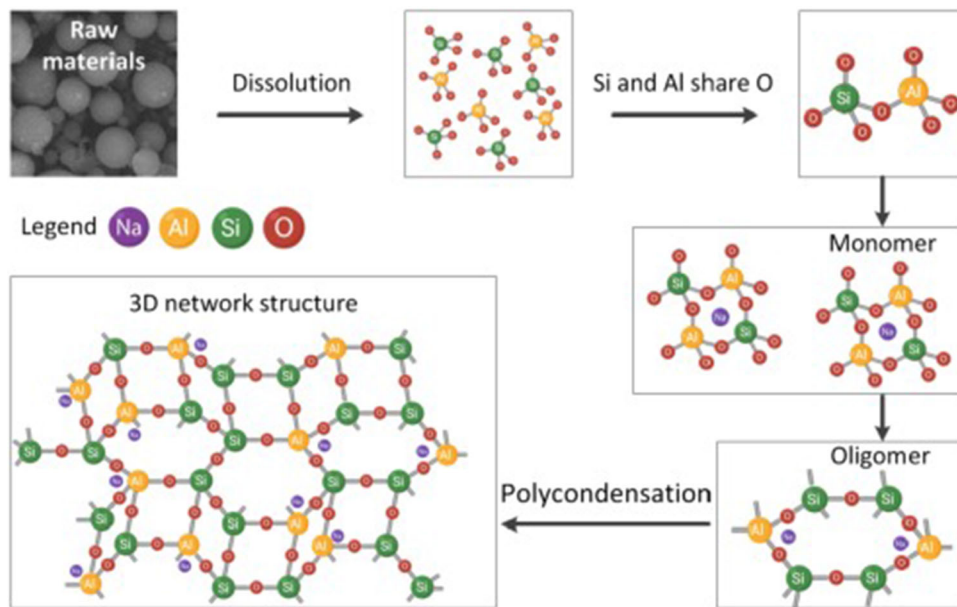
·OH	Hydroxyl radicals
AOP	Advanced oxidation processes
BA	Bottom ash
BC/GM	Biochar/geopolymer
BFS	Blast furnace slag
BT	Bauxite
CB	Carbon black
CC	Calcium carbonate
CGP	Catalytic geopolymer
CTAB	Cetyl-trimethylammonium bromide
EPR	Electron paramagnetic resonance
FA	Fly ashes
FS	Fumed silica
GP	Geopolymer
GPA	Geopolymeric adsorbents
GPM	Geopolymer membrane
HT	Halloysite
HZ	Hydroxysodalite zeolite
KT	Kaolinite
LT	Laterite
MGP	Magnetic geopolymer
MK	Metakaolin
MS	Magnesium slag
PT	Perlite
POFA	Palm oil fuel ash
SF	Silica fume
QZ	Quartz
SMS	Silicomanganese slag
SS	Steel slag

Introduction

Geopolymers are inorganic polymers produced by the polycondensation of aluminosilicate materials, which is promoted by an alkali activator [1]. The reaction consists of three main steps: dissolution, gelation and polycondensation [2]. The reaction begins by the dissolution of the aluminosilicates, which occurs due to hydrolysis (water consumption) of the alkali solution, which forms two distinct monomeric tetrahedral structures: aluminates (AlO_4) and silicates (SiO_4). It is important to point out that geopolymerization is assumed to occur as a consequent dissolution of solid particles at the surface, leading to the release of aluminate and silicate to the solution [3]. These tetrahedral units then begin to link by sharing oxygen atoms, forming polymeric bonds of Si–O–Al–O, resulting in a complex mixture of silicates, aluminates and aluminosilicates. The solution is quickly supersaturated with formed oligomers, leading to a gel formation. Finally, the oligomers condense and eliminate water, developing large network structures, producing an amorphous or semi-crystalline geopolymer, which presents an equilibrium of both negative (Al) and positive (Na) charges [3–6]. A schematic mechanism is presented in Fig. 1.

The great interest in geopolymers research is due to the lower cost of the sources used for their synthesis (such as industrial wastes) and more environmentally friendly production techniques, combined with the

Figure 1 Simplified mechanism of geopolymerization. Reprinted with permission from [7]. Copyright 2020 Elsevier.



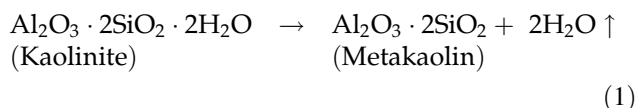
possibility to customize their properties to the application of the final material [8, 9]. Among the characteristics of geopolymers, when compared to Portland cement, stand out: their greater mechanical properties (such as compressive, tensile and flexural strengths, elastic performance and fracture failure), fire-proof and better thermal resistance, chemical inertness, improved resistance to carbonation and frosting, greater durability and less shrinkage during drying [7, 10–12].

There are several recent review articles about the geopolymeric materials discussing general properties, chemistry, possible raw materials and applications [2, 7, 13–21]. Moreover, innovative applications in water and wastewater treatment have been proposed with promisor results in separation processes (adsorption/ion exchange, filtration media and membranes), oxidation processes (peroxidation, ozonation, photocatalytic degradation) or combined processes. Therefore, in this review article, we present a critical panorama about geopolymer uses in separation and reaction processes for water and wastewater treatment.

Most of GP-based materials are based on alkali-activated metakaolin (MK), different types of fly ash (FA), blast furnace slags (BFS) or industrial solid wastes. As the composition and microstructure of these aluminosilicates vary in a wide range, the adsorptive capacity, the textural characteristics or mechanical strength vary widely as well [7, 22].

Recent important reviews describe the effect of the source material and curing conditions on the geopolymer characterization [7, 9, 23–25]. However, they did not emphasize the potential applications and drawbacks in membrane separation processes, catalytic membrane applied in advanced oxidation processes or adsorptive processes for water and wastewater treatment.

Metakaolin (MK) is produced by the calcination of kaolinite (KT) at 600–700 °C, which leads to a dehydroxylation of kaolinite (Eq. 1) [26]. MK has been largely applied in GP synthesis, since it has a higher purity than other aluminosilicate materials, such as fly ash [27]. Furthermore, MK is an appropriate source for producing zeolite-like materials, which are promising for application in filtration membranes, due to combined high mechanical strength and elevated adsorptivity [28]. In addition, Rasaki et al. [2] reinforce that MK-based geopolymers may have small particle sizes, high surface area, nanostructure surfaces and effective electron transference, enabling them suitable for use as catalysts or for co-catalyst support.



Moreover, fly ashes (FA), bottom ashes (BA), palm oil fuel ash (POFA) and blast furnace slags (BFS) have

also attracted attention alone or incorporated into GP, due to their low cost (considered a hazardous industrial waste) and appropriate chemical composition. Moreover, Gollakota et al. [23] point out the fineness of FA provides a higher glass phase, therefore generating a greater geopolymerisation rate, thus producing materials with greater mechanical strength properties. Several high-strength values have been reported for FA-based GP, up to 65 MPa [9, 25, 29]; this is very relevant for applications as concretes/cement, adsorbents and filtration membranes, which can be exposed to elevated pressures. In addition, this kind of waste has already been applied to several different wastewater treatments, to serve as coagulants, adsorbents, membrane filters, Fenton catalysts and photocatalysts [30]. Although, it is worth mentioning that the chemical composition of each type of ash can vary significantly, therefore needing attention on synthesis, in order to produce homogeneous materials [29].

However, the incorporation of some non-conventional sources has also been recently focused on, such as: pozzolan [31], glass [10], natural zeolites [11], biomass fly ash [32], silicomanganese fume [33], magnetite [34], red mud [35] and others. It is important to emphasize that the incorporation of industrial wastes not only can benefit the GP's overall properties, but also has financial and environmental advantages. The choice of these sources will be influenced by availability, cost and application [9, 36].

Si et al. [10] were able to incorporate significant amounts of waste glass powder (up to 20%) in metakaolin-based geopolymers. The authors found that the increase in this waste led to denser microstructure formation, as well as a smaller porous range distribution, with a well-defined pore diameter peak of 30 nm. In addition, a sample with 10% of waste glass powder remarkably decreased the water loss rate under drying conditions, i.e., it reduced drying shrinkage of the synthesized materials.

Moreover, Rossato et al. [34] synthesized a novel magnetic geopolymer (MGP) by adding 5% of magnetite (Fe_3O_4) to its composition (Fig. 2), this facilitated separation of the solids from the solution with a magnet. The authors also reported impressive adsorption capacity (400 mg g^{-1}) of acid green 16 dye (300 mg L^{-1}), although catalytic activity in this process has not been evaluated. Magnetite has interesting catalytic activity on many AOP [37–39]; however, a GP based on this material has not yet been

studied, thus their behavior in these reactions remains unknown.

Similarly, red mud, which is rich in Al and Fe, has been widely investigated as a catalyst to AOP, for example, as a substitute for Fe^{2+} ions in Fenton-like reactions. Although GP preparations with red mud have not focused on these types of reactions [40]. Hu et al. [35] investigated the role of Fe species during geopolymerization and observed that the binding energies of Al–O and Si–O increased; due to Fe^{3+} replacement by Al^{3+} in the geopolymer matrices. Thus, the fabricated materials showed a potential catalytic application and may also reduce leaching, since the Fe atoms are arranged in the GP's network.

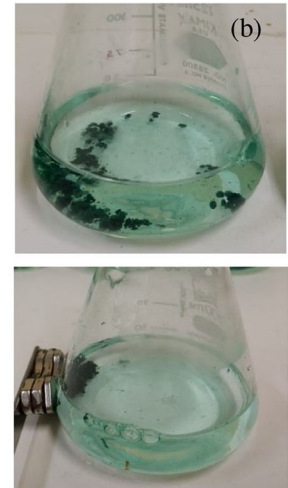
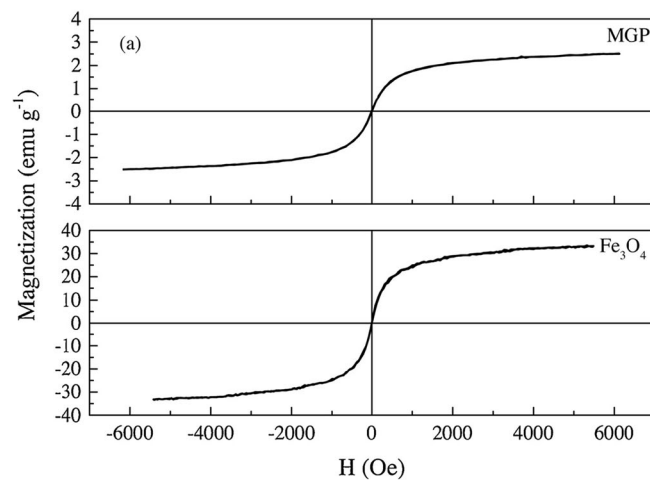
Furthermore, the activity of the geopolymer is highly associated with the aluminosilicate sources, as is their chemical composition, soluble Si/Al content, particle size, presence of inert particles and glass phase (which is inert in water, requiring the addition of an activator for geopolymerization) [41].

Several alkaline activators can be applied to geopolymerization processes; as consequence of the cations different sizes and charges density, distinct properties are obtained in the final material. Commonly hydroxides (NaOH or KOH) and silicates (Na_2SiO_3 or K_2SiO_3) or a mixture of them are used, because of their lower cost and high efficiency [7]. Normally, K^+ -based activators provide faster solidification than Na^+ , because of their larger ionic radius, although they are also more susceptible to cracking and provide lower porosity [42].

Moreover, Xin et al. [43] showed that concrete GP activated by NaOH and Na_2CO_3 generates more microdefects than that with composed of the combination of NaOH and Na_2SiO_3 , which implies that this mixture produces more suitable materials. Other studies have indicated that the combination of Na_2SiO_3 :NaOH produces materials with higher compressive strength than each activator alone [41, 44]. The adequate concentration of the activators depends on the aluminosilicate sources, but Zhang et al. [7] reviewed 173 studies and found that the most common proportion is 2–2.5 of Na_2SiO_3 :NaOH.

Furthermore, studies have revealed that the concentration of the alkaline activator also influences the final properties of the GP matrix, having an optimum value, like the other precursors. If this value is too low, the dissolution of the aluminosilicates is diminished (few OH^- ions in the medium), while a

Figure 2 Magnetization curves of MGP and Fe_3O_4 (a) and MGP particles when attracted by a magnet (b). Reprinted with permission from Rossato et al. [34]. Copyright 2020 Elsevier.



value that is too high decreases the mechanical properties [45, 46].

As mentioned, GP's microstructure and mechanical properties depend not only on the aluminosilicate sources but also on the composition and concentrations of the alkaline activator, such as, for example, Si/Al , $\text{M}_2\text{O}/\text{H}_2\text{O}$, $\text{M}_2\text{O}/\text{SiO}_2$ and $\text{M}_2\text{O}/\text{Al}_2\text{O}_3$ molar ratios (where M is the corresponding alkaline cation Na^+ or K^+) [36]. Normally, these values follow the parameters Davidovits et al. [47] established as ideal for obtaining high mechanical properties (Table 1).

Another influential parameter are the curing conditions, the chosen temperature and its duration will also modify the GP's mechanical properties. Normally, curing is divided into two periods: heated and room-temperature stages. The heated stage generally occurs at temperatures between 40 and 75 °C for 24 h, in order to initiate the reaction, since higher temperatures are needed to overcome the energetic [48, 49]. Contradictory results have been reported for GP curing temperatures, Aliabdo et al. [50] showed that as temperature increases, compressible strength, tensile strength and elastic modulus initially increase, but decrease after reaching a maximum. Yet, Zhang

et al. [48] found similar behavior for compressible strength, while tensile strength had an initial constant with temperature elevation and then decreased. In terms of curing time, it cannot be too short, because nucleation and crystallization processes are reduced, producing a material with low geopolymerization. However, prolonged periods (normally, more than 48 h) cause the granular semi-crystalline structure to break, leading to dehydration and, consequently, gel constriction [23]. Thus, the heat curing time and temperature need to be optimized for each composition, for example for metakaolin-based GP studies found that maximum strength is obtained at 60 °C for 24 h [51, 52].

Yet, the room-temperature step normally takes 7–28 days and water curing is generally applied if the geopolymer usage would be in wet or submersed areas [7]. Furthermore, GP cured under water have higher absorptivity and porosity, although as a consequence the compressive strength is reduced [53].

It is important to comment on the efflorescence phenomena found during GP curing. Efflorescence occurs due to a high concentration of the alkaline activator applied during the synthesis. The unreacted excess diffuses to the material surface where it reacts with atmospheric CO_2 leading to the formation and accumulation of carbonates on the GP surface [54]. This phenomenon not only changes the geopolymers' appearance, but also their mechanical properties [55]. Thus, strategies are used to minimize efflorescence, such as altering: chemical formulation, particle size, type of activator, additives mixing and hydrothermal cure [56, 57]. An interesting study was conducted by Xue et al. [58], who modified the FA-based GP

Table 1 Proposed oxides ratio for GP formulation. Sources: Davidovits et al. [47]

Molar proportion	Minimum	Maximum
$\text{SiO}_2/\text{Al}_2\text{O}_3$	3.30	4.50
$\text{Na}_2\text{O}/\text{H}_2\text{O}$	10	25
$\text{Na}_2\text{O}/\text{SiO}_2$	0.2	0.48
$\text{Na}_2\text{O}/\text{Al}_2\text{O}_3$	0.80	1.60

surface by coating it with octyltriethylsilane, transforming its surface from hydrophilic to hydrophobic, which reduced the leaching of ions, suppressing the efflorescence.

As a consequence of the impressive characteristics of GP, they have attracted attention in several industries including: construction [12, 29], aeronautics, aerospace, shipbuilding and automotive [59–62], nuclear and oil/gas cementing [63, 64], archaeological research [65], acoustic and thermal insulation [66, 67], ceramics [68, 69], pharmaceuticals [70], gaseous and aqueous effluents treatment (by adsorption, membrane filtration and/or chemical catalysis) [34, 71–73] and many others.

Davidovits [65] suggested an ideal proportion of Si/Al depending on its application (Table 2), which could be expanded considering the most recent advances in the application of geopolymers, as shown.

Due to particular properties, geopolymers are being considered for use in membrane filtration or catalytic reactions. For these applications, some textural and physico-chemical properties must be adjusted, since GPs normally have low porosity and low surface area.

A simple method for increasing porosity is to add a small percentage of a porogenic agent (such as H_2O_2), which generates gaseous products (O_2 and H_2 , for example), leading to a more porous material. Other strategies have been investigated, such as direct gas bubbling, the insertion of a sacrificial filler or by introducing an additive to the GP synthesis. However, these methodologies are not often applied since they are complex, expensive and raise environmental concerns [83].

Geopolymeric adsorbents (GPA)

Many studies have been published emphasizing the application of GPs as adsorbents [21, 69, 83–85], for this reason, this topic will point out the adsorption mechanisms (also very relevant for membrane filtration), but only some highlights about recent achievements in this field will be briefly discussed.

Adsorption processes promote the removal of the contaminants by using the interactions of the contaminants and a solid surface, in this review geopolymers. The molecules bonding may occur by two distinct forms: physisorption or chemisorption, depending on van der Waals or chemical interactions, respectively [2].

In general, the mechanism of heavy metals adsorption on GPA occurs by physisorption, due to electrostatic interactions or ionic exchange properties of the GP surface properties, which facilitate the adsorbent regeneration by simple or steam washing, chemical or thermal treatment, but also generates negative effect to multiple ions adsorption, due to sites competition [2, 84]. The equilibrium of adsorption is frequently described according to the Langmuir model (for toxic metals removal, such as Zn^{2+} , Cu^{2+} , Mn^{2+} , Pb^{2+}) [84] and the adsorptive capacity is comparable to that on natural zeolites [86].

Yet, for other substances, as CO_2 [13, 87] or organic molecules [76, 88, 89] chemisorption has an important role. In fact, Al-Zeer and MacKenzie [76] showed that the chemisorption of pyridine on the Lewis and Brønsted acidic sites on their produced fly ash-based GP contributed on the enhancement to their acylation reactions when compared to other metal-zeolite and metal-mesoporous silicate.

Table 2 Proposed oxides ratio for GP formulation. Sources: [8, 26, 69, 70, 72–82]

Si/Al molar ratio	Application
= 1	Bricks; ceramics; fire protection
1–2	Mortar
1–3	Filtration membranes
1–4	Zeolites; chemical stability in air materials
= 2	Low CO_2 cements and concretes; radioactive and toxic waste encapsulation
2–4	Catalyst support; porous materials; H_2 production
= 3	Fire protection fiberglass composites; Foundry equipment; Heat resistant composites (200–1000 °C); tooling for aeronautical titanium process
> 3	Industrial sealants (200–600 °C); tooling for aeronautics spf aluminum; adsorbents; cements; drug support
20–35	Fire resistant and heat resistant fiber composites; biomaterial

Initially, it is important to mention that most investigations have been conducted with dyes or heavy metals as contaminants, some of which even have superior adsorbent capacity than commercial solids [21, 24, 90]. Extensive and comprehensive reviews have reported several advantages of geopolymeric materials as adsorbents, such as, low cost, high adsorptive and/or ion-exchange capacity and chemical stability [2, 16, 18, 19, 21, 69]. However, as emphasized by Luukkonen et al. [24] other pollutants of interest should also be further evaluated, such as pharmaceuticals, oils and fats, phenolic compounds, micro-pollutants, among others. For example, a remarkable adsorption capacity was found by Siyal et al. [89] in their studies using a geopolymer synthesized with fly ash residues to remove an anionic surfactant (sodium dodecyl benzene sulfonate, SDBS) from water. A maximum removal of 714.3 mg g^{-1} was measured. These results show promising application for the separation of similar surfactants from wastewaters.

Recently, Song et al. [77] concluded that high adsorption played an important role in oil separation during geopolymeric membrane filtration, since the droplets were affected by van der Waals forces and a hydrophobic effect. Additional studies should be performed using real water (ground water, surface water, etc.) and wastewaters where competitive and simultaneous cations/anions, organic pollutants and natural organic matter could affect adsorption efficiency [6].

Although most applications of GP in adsorption processes are focused on liquid phases, recent studies have shown their potential for applications in gaseous phases. An important and emergent application is the removal of CO_2 to avoid the greenhouse effect [87, 91–93]. Minelli et al. demonstrated that their synthesized metakaolin-based geopolymers not only had an adsorption capacity comparable to other materials, but could selectively remove CO_2 , since the adsorption capacity of N_2 or CH_4 are low.

Overall, the literature indicates that GPs have a prosperous future as adsorbents. However, impediments remain to their large-scale application, such as their performance when exposed to several different contaminants (industrial wastewater effluents, for example), long-term durability, reusability, the length of regeneration cycles and other operating conditions, etc.

Geopolymeric membranes (GPM)

Membrane filtration is a technology developed to separate molecules according to their characteristics (chemical, size, hydrophilicity, etc.) (Fig. 3) and is normally driven by a pressure difference, allowing some molecules to pass through the membrane (permeate) while retaining others (retentate) [94–96].

Inorganic membranes have attracted attention due to their advantageous properties: chemical and thermal stability, fouling resistance, mechanical strength and long service life, making them widely applicable, especially those made of ceramic materials [98, 99]. Catalytic membranes have also been developed to enhance removal of contaminants [100], minimize fouling (incrustation accumulation, which reduces transmembrane flow) [101] and provide a self-cleaning material [102].

However, inorganic membranes have a high manufacturing cost and are difficult to model. Thus, geopolymer membrane (GPM) materials offer an opportunity to solve these adversities [73]. Recently, Shao et al. [103] analyzed the fabrication costs of nanofiltration membranes with fly ash-based GPM, which they had synthesized. The authors concluded that the production cost of conventional membranes is over $\$1000 \text{ m}^{-2}$, while for the geopolymeric materials, this cost is reduced to $\$31.8 \text{ m}^{-2}$. They also emphasized that the operational pressure used in the experiments (0.1 MPa) was the lowest level applied among efficient nanofiltration procedures.

Moreover, Bai and Colombo [69] and Zhu et al. [104] highlight that GPs, especially porous ones, are promising low-cost materials for use in technological applications, such as adsorbents, catalyst supports or filtration membranes for liquids or gases.

There has been an increasing amount of studies involving GPMs and their new applications (Table 3). One application that should be highlighted is separation by pervaporation; a process that has been used for water desalination and ethanol purification. GPMs are suitable for this procedure due to their high thermal resistance and long durability.

GPMs have also been investigated for several environmental applications such as, air depollution, oil/water separation, as well as the removal of organic pollutants and heavy metals (Table 3). Shao et al. [103], for example, studied fly ash-based GPM in the filtration of several dyes and pharmaceuticals, obtaining impressive separations (greater than 95%).

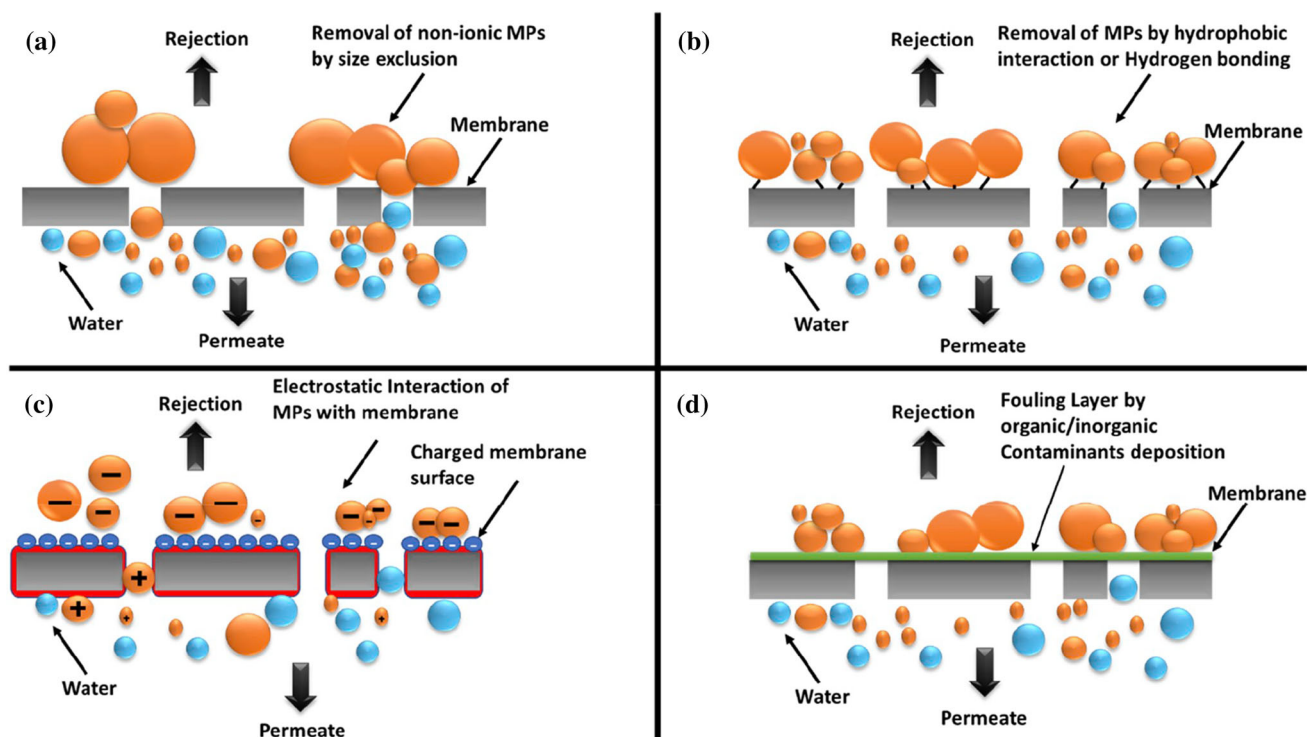


Figure 3 Membrane filtration removal mechanisms: **a** size exclusion, **b** hydrophobicity, **c** electrostatic interaction and **d** adsorption. Reprinted with permission from Khanzada et al. [97]. Copyright 2020 Elsevier.

Geopolymer-based membrane micro-, ultra- and nanofiltration

This section reviews the most important applications of GPMs to aqueous solution filtration. The results are summarized in Table 4. As can be seen, the majority of GPM studies synthesized flat ultraporous membranes. The work of Li et al. [131] is an exception because they produced a membrane composed mainly of nanopores (< 2 nm), not only did the produced material reject 99% of Cd^{2+} ions, but its operating pressure was also relatively low compared to the other studies examined. In terms of the operating pressure of the GPM, He et al. [130] reported the lowest condition. They applied 10 kPa to a fly ash-based geopolymer membrane and were able to remove 91% of Cr^{4+} cations. However, due to the small average pore sizes (12 nm) and the low applied pressure, this study also presented one of the lowest permeate fluxes. The sufficient and suitable compressive strengths (≥ 10 MPa) of GPM enable them to be used in filtration processes [28, 103, 115, 123, 130].

Furthermore, high separation efficiency can be achieved using GPM. Xu et al. [127] studied the

retention of suspended solids in the green liquor stream (Fig. 4) (from the paper industry) by micro-filtration (all pores < 0.28 μm) and found a rejection of $\sim 100\%$, reducing their concentrations from 186 to 0.79 mg L^{-1} , which is far below the requirements for green liquor recycling (< 20 mg L^{-1}).

The applicability of FA-based membranes to remove turbidity, color and suspended solids from produced water [124] and household wastewater [125] was recently reported by Naveed et al. (2019). Besides, significant rejection rate from oils present in the produced water was acquired (78%), reducing its initial very high value (597 mg L^{-1}) [125].

Another relevant issue is the application of GPMs for the removal of dyes or heavy metals from water and wastewater (Table 4). Shao et al. [103] and Song et al. [77] reported especially interesting studies, since they examined not only the types of molecules mentioned, but also the removal of other refractory organic compounds (tetracycline, p-nitrophenol, tetracycline and polystyrene) and water/oil separation (hexadecane). All the results showed high removals ($\geq 97\%$) of the contaminants, except for p-nitrophenol (61%), because of its low molecular size [103].

Table 3 Geopolymers and their application in water and wastewater treatment

Geopolymer base	Application	References
Metakaolin (MK)	–	[105]
Fly ash (FA)	Textile wastewater treatment	[106]
Metakaolin (MK) and hydroxysodalite zeolite (HZ)	Desalinization by pervaporation	[107]
Fly ash (FA)	Water permeation	[108]
Fly ash (FA)	Oil separation from water	[109]
Al ₂ O ₃ –SiO ₂ powder	Desalinization by pervaporation	[110]
Metakaolin (MK) and fumed silica (FS)	Ion exchange	[111]
Metakaolin (MK)	Water permeation	[112]
Metakaolin (MK)	Ethanol/water separation by pervaporation	[113]
Metakaolin (MK)	Heavy metals removal	[73]
Fly ash (FA)	Oil separation from water	[114]
Metakaolin (MK)	Water permeation and turbidity removal	[115]
Blast furnace slag (BFS)	Ethanol/water separation by pervaporation	[116]
Fly ash (FA) and bauxite (BT)	Oil separation from water	[117]
Fly ash (FA), quartz (QZ) and calcium carbonate (CC)	Oil separation from water	[118]
Fly ash (FA)	–	[119]
Metakaolin (MK)	–	[120]
Metakaolin (MK)	Water desalination	[121]
Blast furnace slag (BFS)	Oil separation from water	[122]
Al ₂ O ₃ –SiO ₂ powder	Ethanol/water separation by pervaporation	[123]
Metakaolin (MK) and chitosan	Ion exchange	[62]
Metakaolin and fly ash (FA)	–	[28]
Fly ash (FA)	Household wastewater treatment	[124]
Fly ash (FA)	Produced water treatment	[125]
Metakaolin (MK)	Air particulate matter removal	[126]
Metakaolin (MK)	Water and pulp-papermaking green liquor treatment	[127]
Metakaolin (MK) and fumed silica (FS)	Water desalination	[128]
Metakaolin (MK) and fumed silica (FS)	Organic pollutants removal	[71]
Fly ash (FA), quartz (QZ) and calcium carbonate (CC)	Poultry slaughterhouse wastewater treatment	[129]
Fly ash (FA)	Heavy metals removal	[130]
Metakaolin (MK) and fumed silica (FS)	Heavy metals removal	[131]
Fly ash (FA) and faujasite	Low-temperature solid oxide fuel cells	[132]
Metakaolin (MK)	Antimicrobial, AOP and membrane filtration	[133]
Fly ash (FA)	Adsorption and organic pollutants removal	[103]
Metakaolin (MK) and chitosan	Water permeation, oil separation from water, heavy metals and organic pollutants removal	[77]
Laterite (LT)	Ethanol/water separation by pervaporation	[134]
Blast furnace slag (BFS) and ground mixed recycled aggregates	–	[6]

Moreover, distinct mechanisms were observed for the contaminants removal. Several researches describe the main pathway for the pollutants rejections as a combination of adsorption kinetics with sieve segregation [71, 73, 127, 131], i.e., molecules (larger than the membranes pores) are barred due to

size exclusion, simultaneously with molecules bonding into the surface, due to their interactions affinity. Besides, electrostatic interactions were also considered important on membranes filtration [77, 130], Song et al. [77] proposed that organic cationic molecules (crystal violet) and heavy metal ions were

Table 4 GPM applied to micro-, ultra- and nanofiltration

Geopolymer base	Membrane diameter, mm	Membrane thickness/length, mm	Pore diameter, mm	Pressure operation, kPa	Flux, $\text{kg m}^{-2} \text{h}^{-1}$	Retentate	Permeate	Removal, %	References
FA	5	150	250	100	90	Suspended particles and dye	Water	99 and 90	[106]
FA	5.5	100	900	100	17000	–	Water	–	[108]
FA	55	100	770	100	2270	Oil	Water	~ 100	[109]
MK	–	–	135	1	13.5	–	Water	–	[112]
MK	40	10	276	100	99	Ni^{2+}	Water	96	[73]
FA	55	5	1200	138	80	Oil	Water	99	[114]
MK	20	5	20–100	100	60	Turbidity	Water	~ 100	[115]
FA/BT	20	2	480	50	46	Oil	Water	98	[117]
FA/QZ/CC	55	5	1360	69	121	Oil	Water	~ 100	[118]
BFS	12	–	660	220	1960	Gas oil	Water	~ 100	[122]
FA	50	5	6600	200	43	Suspended particles, oil and detergents	Water	Not specified	[124]
FA	50	5	250	300	14	Suspended solids	Water	78	[125]
MK	20	0.5	90	200	245	Suspended solids	Green liquor (papermaking)	~ 100	[127]
MK/SF	40	4	30	90	40	Green dye	Water	~ 100	[71]
FA/QZ/CC	5.5	100	133	414	24	Suspended particles and oil	Water	~ 100	[129]
FA	40	6	12	10	8	Cr^{+3}	Water	91	[130]
MK/SF	40	10	< 2	40	42	Cd^{2+}	Water	99	[131]
MK	100	0.1	763000	Not specified ^a	Not specified ^a	–	Water	–	[133]
FA	10	0.05	30–2000	98	425	Methylene blue	Water	97	[103]
					380	Rhodamine B		98	
					410	Congo red		98	
					380	Tetracycline		99	
					440	p-Nitrophenol		61	
					370	Oxytetracycline		99	
MK/chitosan	0.001	0.001	15	80	3–4	Congo red	Water	99	[77]
						Crystal violet		99	
						Hexadecane		~ 100	
						Polystyrene		98	
						Cu^{2+}		99	

Table 4 continued

Geopolymer base	Membrane diameter, mm	Membrane thickness/length, mm	Pore diameter, mm	Pressure operation, kPa	Flux, $\text{kg m}^{-2} \text{h}^{-1}$	Retentate	Permeate	Removal, %	References
						Pb^{2+}		98	

^aValues were presented in terms of permeability

attracted by the negatively surface of the GP, being easily removed. At the same time, the authors concluded that, for congo red and crystal violet dyes removal, chelation or hydrogen bonding (hydrophilicity) also had important participation, once the existence of amino, hydroxyl and carboxyl groups on their produced GP facilitated the molecules bonding.

Thus, the reviewed studies showed promising results in terms of pollutants separation efficiency permeate flow/operational pressure relationship, ultra- and nanoporous distribution, versatile removal mechanisms, aside from having low cost and easy production. These results are thus of great interest for further research and possible commercial applications.

Geopolymer-based catalysts

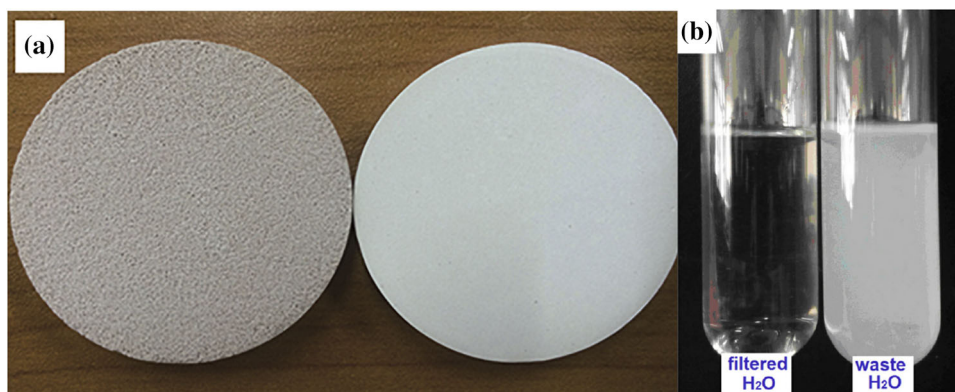
Catalytic geopolymers (CGP) are geopolymers that are functionalized and/or modified to enhance specific reaction kinetics. Mechanical strength, thermal stability, acid-basic properties, permeability and durability are some of the properties for which they are used in catalysis, as catalysts themselves or as catalyst support [83, 135].

Furthermore, the microstructure and morphology of CGPs are also interesting, given that some authors have synthesized GPs with structures similar to zeolites (in terms of surface area, pore size and volume, number of active sites, affinity for reactants and stability) (Fig. 5), which are widely studied for their applications in catalysis [21, 74, 136].

As explained above, during polycondensation, tetrahedral silicates and aluminates connect randomly and, some cations (Na^+ , K^+ and Ca^{2+}) simultaneously interact with them, promoting an electronic balance. Thus, in some studies, these cations are substituted by other transition metal and/or rare metal cations to produce CGPs with enhanced activity [85].

The most common methods for incorporating these metals in the GP are ion exchange, surface coating/impregnation, incorporation into the composition during synthesis and thermal activation. These treatments alter the materials' porosity, surface area, available active sites, band gap, electronic surface charge and many other properties, which improve their catalytic activity [2, 85].

Figure 4 Support (left) and inorganic composite membrane (right) (a); and green liquor before and after filtration (b). Reprinted with permission from Xu et al. [127]. Copyright 2019 Elsevier.



Few studies have been done with CGP, a search in SCOPUS with the words *catalytic AND geopolymer* yielded only 54 results in the past 10 years. Although there was a sharp increase, in 2019 when 11 studies were published ($\sim 20\%$) [137]. Some of the publications on CGP are listed in Table 5.

In a very recent work, Chen et al. [71] demonstrated that the incorporation of Cr_2O_3 not only enhanced the membrane flux (compared to an undoped process) with high rejection ($\sim 100\%$), but also presented low fouling during the filtration process. Moreover, the incorporation of the catalyst led to a high photocatalytic performance for the degradation of green dye (30 mg L^{-1}), and almost complete oxidation was obtained in 100 min.

Considering the studies reported in the literature (Table 5), geopolymer-based catalytic membranes are promising, since they combine adjustable porosity, diverse morphology, easy modulation, excellent mechanical and thermal properties and are simple to prepare, environmentally friendly and have lower manufacturing costs.

Similarly to the application of CGP as membranes, the main advantage of using these materials for catalyst support is their mechanical and thermal characteristics, as well as high surface area, porosity and, in some cases, photo-activity, which increase interest in these materials [69, 72]. Asim et al. [85] emphasize that the surface modification of geopolymers is beneficial to their catalytic applications.

Several of the studies cited (Table 5) used a catalyst supported in GP for organic syntheses reactions. Alzeer and MacKenzie [166] reported that the CGP produced (with NH_4^+ ion exchange) had superior catalytic activity than other commonly used aluminosilicate supports such as zeolite M and mesoporous molecular sieves.

The production of H_2 has also been studied through the application of CGP materials (Table 5), mainly by the incorporation of metal oxides (CeO_2 , CuO , $\text{In}_2\text{O}_3\text{-NiO}$, CaWO_4) or graphene as photocatalysts. These materials are able to act as electron acceptors and improve the catalytic performance of geopolymers, consequently raising the reaction rate.

Zhang et al. [176] studied both H_2 production and dye removal using ZnO /graphene CGP. The H_2 yield was up to 30% higher due to the incorporation of ZnO , because of the synergistic effects of this semiconductor with graphene and the geopolymer composition itself. Zhang et al. [176] also noted a

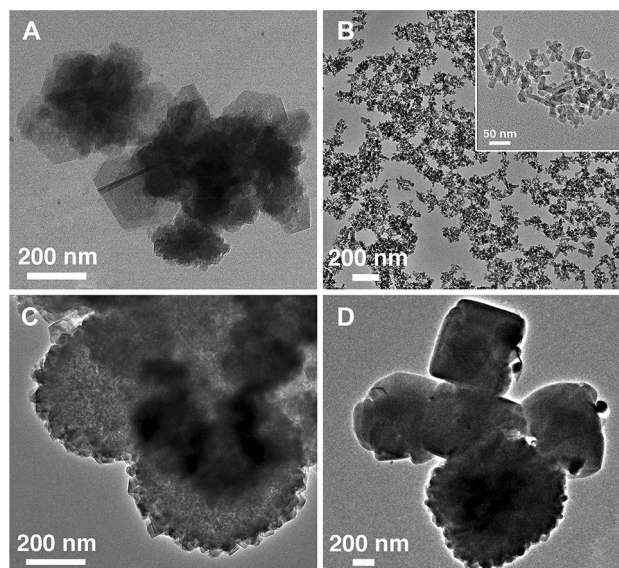


Figure 5 Nano-geopolymeric zeolites, where the aluminosilicate source is: faujasite (a), cancrinite (b), sodalite (c) and Linde-Type A (d). Reprinted with permission from Chen et al. [74]. Copyright 2019 American Chemical Society.

Table 5 Summary of geopolymer-based catalysts and their application

Geopolymer base	Catalyst	Application	References
Metakaolin (MK)	TiO ₂	Photocatalysis	[138]
Metakaolin (MK)	TiO ₂	Adsorption and photocatalysis	[139]
Metakaolin (MK) and blast furnace slag (BFS)	NH ₄ ⁺ , Co ²⁺ , Cu ²⁺ , Fe, or Pt	Redox reactions	[140]
Metakaolin (MK)	NH ₄ ⁺ and TiO ₂	Adsorption and photocatalysis	[141]
Steel slag (SS)	NH ₄ ⁺ or Ni ²⁺	Adsorption and photocatalysis	[142]
Fly ash (FA)	Fe ₂ O ₃ (from raw materials)	Adsorption and photocatalysis	[143]
Blast furnace slag (BFS)	Fe ₂ O ₃	Adsorption and photocatalysis	[144]
Metakaolin (MK)	TiO ₂	Adsorption and photocatalysis	[145]
Blast furnace slag (BFS)	Fe ₂ O ₃ and TiO ₂ (from raw materials)	H ₂ production	[146]
Magnesium slag (MS)	NH ₄ ⁺ and CuO	H ₂ production	[147]
Fly ash (FA)	Ag	Antimicrobial	[49]
Metakaolin (MK)	Ni	Ethanol reforming, autothermal reforming and partial oxidation	[148]
Kaolinite (KT)	Cu ₂ O/TiO ₂	Adsorption and photocatalysis	[149]
Metakaolin (MK)	CuCl ₂	Antimicrobial	[150]
Steel slag (SS)	Composition from the raw materials	Photocatalysis	[151]
Metakaolinite (MKT)	Ca ²⁺	Biodiesel production	[152]
Magnesium slag (MS)	NH ₄ ⁺ or CuO/NiO	Adsorption and photocatalysis	[153]
Halloysite (HT)	NH ₄ ⁺	Beckmann rearrangement reaction	[154]
Fly ash (FA)	TiO ₂	Mechanical properties enhancement	[155]
Kaolinite (KT) and cetyltrimethylammonium bromide (CTAB)	Cu ₂ O/TiO ₂	Adsorption and photocatalysis	[72]
Steel slag (SS)	NH ₄ ⁺ or CeO ₂	Adsorption and photocatalysis	[156]
Al ₂ O ₃ –SiO ₂ powders	CdS	Adsorption and photocatalysis	[157]
Metakaolin (MK) and fly ash (FA)	TiO ₂	Adsorption and photocatalysis	[158]
Blast furnace slag (BFS)	Graphene	Adsorption and photocatalysis	[159]
Halloysite (HT)	NH ₄ ⁺	Friedel–Crafts alkylation	[160]
Metakaolin (MK)	Ag	Antimicrobial	[161]
Metakaolin (MK) and fly ash (FA)	TiO ₂	Photocatalysis	[75]
Metakaolin (MK)	ZnO	Antimicrobial	[27]
Steel slag (SS)	NH ₄ ⁺ or CeO ₂	H ₂ production	[162]
Bottom ash (BA)	NH ₄ ⁺ or Mn ²⁺ –CuO/graphene	Photocatalysis and H ₂ production	[78]
Fly ash (FA)	NH ₄ ⁺ or In ₂ O ₃ –NiO	H ₂ production	[163]
Blast furnace slag (BFS)	CaWO ₄	H ₂ production	[164]
Blast furnace slag (BFS)	NH ₄ ⁺ or CaWO ₄ /CaSiO ₃ ·H ₂ O	Photocatalysis	[165]
Fly ash (FA)	NH ₄ ⁺	Friedel–Crafts benzoylation	[166]
Metakaolin (MK)	Cu, Ni or Cu/Ni	Isopropanol dehydrogenation	[167]
Metakolin (MK)	Composition from the raw materials	Biodiesel production	[168]
Fly ash (FA)	ZnO–SiO ₂	Antimicrobial	[169]
Steel slag (SS)	NH ₄ ⁺ or CdO/graphene	Photocatalysis	[170]

Table 5 continued

Geopolymer base	Catalyst	Application	References
Silicomanganese slag (SMS)	Carbon black (CB)	Photocatalysis	[171]
Fly ash (FA)	Graphene	Adsorption and photocatalysis	[172]
Blast furnace slag (BFS)	Graphene	H ₂ production	[173]
Fly ash (FA)	NH ₄ ⁺	Friedel–Crafts acylation	[76]
Metakaolin (MK)	Fe ₂ O ₃ , Mn ₂ O ₃ or Fe ₂ O ₃ / Mn ₂ O ₃	Biomass gasification	[174]
Silicomanganese slag (SMS)	NH ₄ ⁺ or CaMoO ₄	Adsorption and photocatalysis	[175]
Blast furnace slag (BFS)	ZnO/grapheme	Photocatalysis and H ₂ production	[176]
Fly ash (FA)	La _{0.6} Sr _{0.4} Ga _{0.3} Fe _{0.7} O ₃ (from raw materials)	CH ₄ conversion	[177]
Metakaolin (MK) and silica fume (SF)	Cr ₂ O ₃	Photocatalysis and membrane filtration	[71]
Metakaolin (MK) and blast furnace slag (BFS)	Alkaline lignin	Adsorption and Fenton-like process	[178]
Metakaolin (MK)	Ag ⁰ , Ag ⁺ , Cu ⁺ and Cu ²⁺	Antimicrobial, AOP and membrane filtration	[133]
Fly ash (FA)	TiO ₂	Photocatalysis	[179]
Metakaolin (MK)	K ₂ CuFe(CN) ₆	Adsorption	[180]
Metakaolin (MK)	Fe ₃ O ₄	Adsorption	[34]
Perlite (PT)	Fe ₂ O ₃ (from raw materials)	Adsorption and photocatalysis	[88]
Blast furnace slag (BFS)	Ni ²⁺	CO ₂ methanation	[181]
Si-doped with carbon nanotubes (simulation)	Graphene	Mechanical properties enhancement	[182]

considerable separation of photo-generating e⁻/h⁺ pairs, promoting efficient reduction reactions. Moreover, they observed that an incorporation of 15 wt% of ZnO to the geopolymer enhanced the degradation kinetics constant by approximately 17 times, possessing a high activity under visible light.

Moreover, the majority of the studies utilized CPG in photocatalysis (Table 5), promoted high oxidation of dyes, volatile molecules and nitrogen oxides [34, 71, 72, 143, 157, 158]. Metal oxides, metal alloys and sulfides were used to coat GP and enhanced their absorbance under visible light [78, 148, 157]. Ancora et al. [139] and Chen et al. [75] reported impressive photocatalytic performance not only on the surface, but also in the bulk of the material, as a consequence of its high porosity.

As seen above, the chemical composition, porosity and water adsorption make geopolymers suitable for other AOP reactions as catalysts or for catalyst support, a still little explored field. Studies that applied CGPs for these purposes will be discussed below.

Geopolymer-based catalysts applied to advanced oxidation processes

Initially, it is important to point out that some authors did not introduce catalysts to their geopolymeric materials (Table 6), showing photocatalytic activity due to the composition of raw materials used in their synthesis [88, 143, 151]. These three studies found a high degradation of dye compounds ($\geq 96\%$) when exposed to UV light, which is attributed in particular to the presence of Fe₂O₃ in their composition, a widely studied semiconductor, since it is rapidly excited by electron transfer and has a relatively low band gap [183].

In addition, only one CGP has been applied to a Fenton-like reaction (Table 5), all of the other studies focused on photocatalysis. Huang et al. [178] produced a biochar/geopolymer composite membrane (denominated as BC/GM), coated with alkaline lignin, which was simultaneously carbonated and self-activated. It was applied to a highly oxidizing reaction in the presence of H₂O₂ (a Fenton-like process). Pharmaceutical tetracycline (50 mg L⁻¹) was almost completely degraded with 150 mg L⁻¹ of the GP (10 mL L⁻¹ H₂O₂, pH 5.0, 60 °C, 5 h). Moreover, electron paramagnetic resonance (EPR) analysis

Table 6 Photocatalytic and Fenton-like degradation results by catalytic geopolymers application

Geopolymer base	Catalyst dosage, wt%	Band gap, eV	Light source λ , nm; power, W	Pollutant concentration, mg L ⁻¹	Reaction time, min	Removal, %	References
MK	TiO ₂ (3)	–	–	NO	60	97	[139]
MK	TiO ₂	–	UV/Vis; 900	Methylene blue	90	~ 100	[141]
SS	Ni ²⁺ (7)	–	254; 40	Methylene blue (1283)	350	94	[142]
FA	Fe ₂ O ₃ (5; from raw materials)	–	254; 40	Congo red (6)	100	~ 100	[143]
BFS	Fe ₂ O ₃ (5)	–	254; 40	Methylene blue (1283)	20	93	[144]
MK	TiO ₂	–	365; 15	2-butanone (5)	5000	10	[145]
KT	Cu ₂ O/TiO ₂ (30)	2.17	UV; 150	Methylene blue (1000)	60	98	[149]
SS	Composition from raw materials	–	UV; 18	Malachite green (4)	60	96	[151]
KT and CTAB	Cu ₂ O/TiO ₂	–	UV;150	Methylene blue (320)	960	97	[72]
CC	CeO ₂ (8)	2.41	UV; 18	Malachite green (8)	70	~ 100	[156]
Al ₂ O ₃ –SiO ₂ powders	CdS (13)7	–	245; 8	Methyl orange (5000)	110	93	[157]
FA	TiO ₂ (3)	–	UV; 9	NO (7.5·10 ⁻⁵)	–	~ 100	[158]
BFS	Graphene (0.02)	–	UV; 18	Methyl violet (4)	110	91	[159]
MK and FA	TiO ₂	–	254; 8 (4 lamps)	Methylene blue (10)	480	70	[75]
BA	Mn ²⁺ –CuO/graphene	–	365; 18	Sky blue 5B (20)	90	~ 100	[78]
BFS	CaWO ₄ (5)	–	365; 18	Violet 5BN (4)	70	90	[165]
SS	CdO/Graphene (8)	2.87	UV; 18	Direct fast bordeaux dye (30)	100	~ 100	[170]
SMS	CB (4.5)	2.53	365; 18	Basic violet 5BN (4)	100	88	[171]
FA	Graphene (1)	3.20	253; 30	Indigo carmine (10)	90	90	[172]
SMS	CaMoO ₄ (4)	–	UV; 18	Basic violet 5BN (6)	90	~ 100	[175]
BFS	ZnO/graphene (15)	3.20	320–780; 300	Basic violet 5BN (4)	120	93	[176]
MK and SS	Cr ₂ O ₃ (5)	–	Xenon lamp	Basic green (30)	100	~ 100	[71]
MK and BFS	Alkaline lignin	–	–	Tetracycline (30)	300	~ 100	[178]
FA	TiO ₂ (5)	–	Xenon lamp; 300	Methylene blue (20)	90	95	[179]
PT	Fe ₂ O ₃ (0.9; from raw materials)	3.82	254–380; 125	Methylene blue (30)	240	98	[88]

revealed the formation of a hydroxyl radical ($\cdot\text{OH}$) by solid materials. The authors concluded that graphitized carbon, ketone, quinone moieties and defect structures contributed to the generation of radicals. The proposed reaction mechanism is presented in Fig. 6.

As expected, the catalyst most commonly added to photocatalytic GP is TiO₂ (Table 6). The reported results showed a lower degradation or a higher reaction time than other studies that utilized distinct

catalysts, probably a consequence of TiO₂'s high band gap (~ 3.20 eV).

To overcome this difficulty, Falah et al. (2015) [149] used the Cu₂O/TiO₂ heterojunction in the synthesized CGP, producing a material with a reduced band gap of 2.17 eV, which led to high removal of methylene blue (1000 mg L⁻¹, 98%). The incorporation of other metal oxides was also studied by Kang et al. [156], Zhang et al. [170] and Chen et al. [71] (CeO₂, CdO/graphene and Cr₂O₃ respectively) and showed an almost complete degradation of three

Figure 6 Schematic mechanism of $\cdot\text{OH}$ radicals formation and tetracycline degradation. Reprinted with permission from Huang et al. [178]. Copyright 2020 Elsevier.

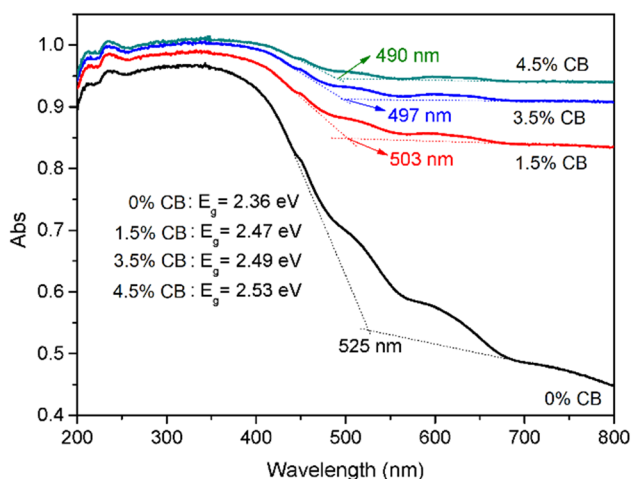
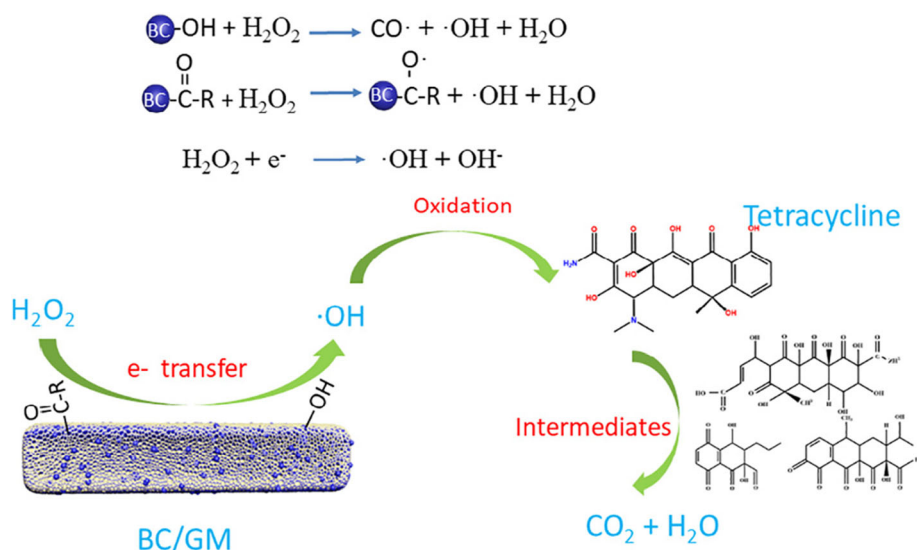


Figure 7 UV–Vis diffuse reflectance spectra of the samples with different amounts of CB. Reprinted with permission from Zhang et al. [171]. Copyright 2018 Multidisciplinary Digital Publishing Institute.

different contaminants, malachite green, direct fast bordeaux dye and basic green, respectively.

Moreover, graphene is commonly reported for CGP (Table 5), in general as part of the composite, producing catalysts that act with Z-scheme mechanisms, which enhances photocatalytic activity by promoting electron transfers between the higher conduction band and the lower valence band of each semiconductor, resulting in elevated generation of e^-/h^+ pairs and consequent higher degradation potentials [184].

The work of Zhang et al. [171] also deserves emphasis. These authors incorporated carbon black (CB) into their GP samples, the presence of this compound produced a solid with one of the lowest reported band gaps for CGP (2.53 eV) and also increased the absorption in the visible region (Table 6 and Fig. 7). This is highly associated with the increased electroconductivity of the photocatalysts, improving the e^-/h^+ pair segregation by facilitating transmission to the network of CB.

Unfortunately, studies that only examined TiO_2 semiconductor loading did not calculate the band gap values to provide a better comparison. Actually, few investigations reported this parameter value, 7 of the 26 (Table 6), which is probably because GPs are composed of several materials, making it difficult to estimate it. In addition, the reported values considered the GP to be a pure semiconductor, to facilitate obtaining its value [88].

Furthermore, although few studies were conducted under visible light, their results were promising. Zhang et al. [176], Chen et al. [71] and Maiti et al. [179] observed organic contaminant degradation of 93%, ~ 100% and 95%, respectively. The band gap of CGP used by Zhang et al. [176] is considered high, yet the material demonstrated great photocatalytic efficiency.

It is also important to comment on the mechanical properties of the CGP. Various studies demonstrated enhanced values of compressible strength and flexural modulus [78, 144, 159, 171, 176, 179], many of them even higher than those reported for membrane

filtration applications. Zhang et al. [144, 176], for example, obtained, in this order, 86 MPa and 59 MPa of compressive strength, while the flexural strengths were 2 MPa and 5.2 MPa, respectively. It is known that some compounds such as TiO₂ and graphene are able to increase these properties [155, 182], which make them very interesting for application as catalytic membranes.

The literature review indicated that few studies have applied CGP to photocatalysis or peroxidation and none in another AOP. Moreover, these studies focused mainly on the degradation of dyes, while other pollutants have been little explored. Thus, it is not only important to study CGP performance in other advanced oxidation processes, but also the behavior of other contaminants when submitted to these materials, as emerging contaminants, which have been widely reported to degrade with AOP.

Final remarks

In general, from the results presented in this review of the literature, it can be concluded that geopolymeric materials are promising for a number of their characteristics (compressive and flexural strength, thermal resistance, porosity, water absorption, electronic transference, surface area, catalytic activity, etc.). Thus, they appear as an effective solution for minimizing costs for both membrane filtration and advanced oxidation processes, making them more economically viable. This is not only because of the lower production costs for GPMs, but also due to the fact they possibly need none or lower catalyst loads, as well as shorter time and lower temperature conditions in manufacturing than others adsorbents, inorganic membranes precursors or catalyst supports, such as zeolites.

Therefore, a combination of these processes using catalytic geopolymeric membranes may be used in the future for many applications, including water and wastewater treatments. However, more research is still needed in this field, since few studies have been published that consider large-scale applications. In particular, studies involving other important pollutants, different AOP reactions (aside from photocatalysis), metal leaching, reuse, maintenance costs (replacement of materials, cleaning, fouling, etc.), chemical resistance and synthesis homogeneity (as a consequence of the variability of the industrial waste

samples) would be important to clarify some essential issues that would allow further expanding development of GPMs.

Acknowledgements

The authors would like to thank the Coordination of Improvement of Higher Education Personnel (CAPES - Brazil)/Brazil [Grant Code 001; and CAPES-PRINT Project Number 88887.310560/2018-00] and National Council for Scientific and Technological Development (CNPq - Brazil) [Grant Number 405892/2013 6] for their financial support. ERC is grateful to Project RTI2018-099668-BC22 of the Ministerio de Ciencia, Innovación y Universidades, and project UMA18-FEDERJA-126 of the Junta de Andalucía and FEDER funds.

Authors' contribution

Conceptualization: [DGDR; RFPMM]; writing—original draft preparation: [DGDR; RMP; RAP; ER-C]; writing—review and editing: [DGDR; RMP; RAP; ER-C; RFPMM]; funding acquisition: [RFPMM], project administration: [RFPMM]; supervision: [RFPMM].

Compliance with ethical standards

Conflict of interest The authors declare that they have no conflict of interest.

References

- [1] Davidovits J (1972) Procédé de fabrication de panneaux agglomérés et panneaux résultant de l'application de ce procédé
- [2] Rasaki SA, Bingxue Z, Guarecuco R et al (2019) Geopolymer for use in heavy metals adsorption, and advanced oxidative processes: a critical review. *J Clean Prod* 213:42–58. <https://doi.org/10.1016/j.jclepro.2018.12.145>
- [3] Duxson P, Fernández-Jiménez A, Provis JL et al (2007) Geopolymer technology: the current state of the art. *J Mater Sci* 42:2917–2933. <https://doi.org/10.1007/s10853-006-0637-z>

- [4] Ahmaruzzaman M (2010) A review on the utilization of fly ash. *Prog Energy Combust Sci* 36:327–363. <https://doi.org/10.1016/j.peccs.2009.11.003>
- [5] El-Habaak G, Askalany M, Abdel-Hakeem M (2018) Building up and characterization of calcined marl-based geopolymeric cement. *Infrastructures*. <https://doi.org/10.3390/infrastructures3030022>
- [6] Tan J, Cai J, Li X et al (2020) Development of eco-friendly geopolymers with ground mixed recycled aggregates and slag. *J Clean Prod* 256:120369. <https://doi.org/10.1016/j.jclepro.2020.120369>
- [7] Zhang P, Wang K, Li Q et al (2020) Fabrication and engineering properties of concretes based on geopolymers/alkali-activated binders—a review. *J Clean Prod* 258:120896. <https://doi.org/10.1016/j.jclepro.2020.120896>
- [8] Davidovits J (2002) Environmentally driven geopolymer cement applications. In: *Geopolymer 2002 conference*, pp 1–9
- [9] Mehta A, Siddique R (2016) An overview of geopolymers derived from industrial by-products. *Constr Build Mater* 127:183–198. <https://doi.org/10.1016/j.conbuildmat.2016.09.136>
- [10] Si R, Dai Q, Guo S, Wang J (2020) Mechanical property, nanopore structure and drying shrinkage of metakaolin-based geopolymer with waste glass powder. *J Clean Prod* 242:118502. <https://doi.org/10.1016/j.jclepro.2019.118502>
- [11] Lynch JLV, Baykara H, Cornejo M et al (2018) Preparation, characterization, and determination of mechanical and thermal stability of natural zeolite-based foamed geopolymers. *Constr Build Mater* 172:448–456. <https://doi.org/10.1016/j.conbuildmat.2018.03.253>
- [12] Lahoti M, Tan KH, Yang EH (2019) A critical review of geopolymer properties for structural fire-resistance applications. *Constr Build Mater* 221:514–526. <https://doi.org/10.1016/j.conbuildmat.2019.06.076>
- [13] Tchadjie LN, Ekolu SO (2018) Enhancing the reactivity of aluminosilicate materials toward geopolymer synthesis. *J Mater Sci* 53:4709–4733. <https://doi.org/10.1007/s10853-017-1907-7>
- [14] Assi LN, Carter K, Deaver E, Ziehl P (2020) Review of availability of source materials for geopolymer/sustainable concrete. *J Clean Prod* 263:121477. <https://doi.org/10.1016/j.jclepro.2020.121477>
- [15] Zhang YJ, Han ZC, He PY, Chen H (2020) Geopolymer-based catalysts for cost-effective environmental governance: a review based on source control and end-of-pipe treatment. *J Clean Prod*. <https://doi.org/10.1016/j.jclepro.2020.121556>
- [16] Singh J, Singh SP (2019) Geopolymerization of solid waste of non-ferrous metallurgy—a review. *J Environ Manag* 251:109571. <https://doi.org/10.1016/j.jenvman.2019.109571>
- [17] Mohajerani A, Suter D, Jeffrey T et al (2019) Recycling waste materials in geopolymer concrete. *Clean Technol Environ Policy* 21:493–515. <https://doi.org/10.1007/s10098-018-01660-2>
- [18] Gomes SDC, Zhou JL, Li W, Long G (2019) Progress in manufacture and properties of construction materials incorporating water treatment sludge: a review. *Resour Conserv Recycl* 145:148–159. <https://doi.org/10.1016/j.resconrec.2019.02.032>
- [19] Ji Z, Pei Y (2019) Bibliographic and visualized analysis of geopolymer research and its application in heavy metal immobilization: a review. *J Environ Manag* 231:256–267. <https://doi.org/10.1016/j.jenvman.2018.10.041>
- [20] Singh NB, Nagpal G, Agrawal S (2018) Water purification by using adsorbents: a review. *Environ Technol Innov* 11:187–240. <https://doi.org/10.1016/j.eti.2018.05.006>
- [21] Siyal AA, Shamsuddin MR, Khan MI et al (2018) A review on geopolymers as emerging materials for the adsorption of heavy metals and dyes. *J Environ Manag* 224:327–339. <https://doi.org/10.1016/j.jenvman.2018.07.046>
- [22] Fletcher RA, MacKenzie KJD, Nicholson CL, Shimada S (2005) The composition range of aluminosilicate geopolymers. *J Eur Ceram Soc* 25:1471–1477. <https://doi.org/10.1016/j.jeurceramsoc.2004.06.001>
- [23] Gollakota ARK, Volli V, Shu C (2019) Progressive utilisation prospects of coal fly ash: a review. *Sci Total Environ* 672:951–989. <https://doi.org/10.1016/j.scitotenv.2019.03.337>
- [24] Luukkonen T, Heponiemi A, Runtti H et al (2019) Application of alkali-activated materials for water and wastewater treatment: a review. *Rev Environ Sci Biotechnol* 18:271–297. <https://doi.org/10.1007/s11157-019-09494-0>
- [25] Zhuang XY, Chen L, Komarneni S et al (2016) Fly ash-based geopolymer: clean production, properties and applications. *J Clean Prod* 125:253–267. <https://doi.org/10.1016/j.jclepro.2016.03.019>
- [26] Ferone C, Colangelo F, Roviello G et al (2013) Application-oriented chemical optimization of a metakaolin based geopolymer. *Materials (Basel)* 6:1920–1939. <https://doi.org/10.3390/ma6051920>
- [27] Nur QA, Sari NU, Harianti S (2017) Development of geopolymers composite based on metakaolin-nano ZnO for antibacterial application. *Mater Sci Eng*. <https://doi.org/10.1088/1742-6596/755/1/011001>
- [28] De Rossi A, Simão L, Ribeiro MJ et al (2019) In-situ synthesis of zeolites by geopolymerization of biomass fly ash and metakaolin. *Mater Lett* 236:644–648. <https://doi.org/10.1016/j.matlet.2018.11.016>

- [29] Jindal BB (2019) Investigations on the properties of geopolymer mortar and concrete with mineral admixtures: a review. *Constr Build Mater* 227:116644. <https://doi.org/10.1016/j.conbuildmat.2019.08.025>
- [30] Mushtaq F, Zahid M, Bhatti IA et al (2019) Possible applications of coal fly ash in wastewater treatment. *J Environ Manag* 240:27–46. <https://doi.org/10.1016/j.jenvman.2019.03.054>
- [31] Haddad RH, Lababneh ZK (2020) Geopolymer composites using natural pozzolan and oil-shale ash base materials: a parametric study. *Constr Build Mater* 240:117899. <https://doi.org/10.1016/j.conbuildmat.2019.117899>
- [32] Novais RM, Ascensão G, Tobaldi DM et al (2018) Biomass fly ash geopolymer monoliths for effective methylene blue removal from wastewaters. *J Clean Prod* 171:783–794. <https://doi.org/10.1016/j.jclepro.2017.10.078>
- [33] Nasir M, Johari MAM, Yusuf MO et al (2019) Synthesis of alkali-activated binary blended silico-manganese fume and ground blast furnace slag mortar. *J Adv Concr Technol* 17:728–735. <https://doi.org/10.3151/jact.17.728>
- [34] Rossatto DL, Netto MS, Jahn SL et al (2020) Highly efficient adsorption performance of a novel magnetic geopolymer/Fe₃O₄ composite towards removal of aqueous acid green 16 dye. *J Environ Chem Eng* 8:103804. <https://doi.org/10.1016/j.jece.2020.103804>
- [35] Hu Y, Liang S, Yang J et al (2019) Role of Fe species in geopolymer synthesized from alkali-thermal pretreated Fe-rich Bayer red mud. *Constr Build Mater* 200:398–407. <https://doi.org/10.1016/j.conbuildmat.2018.12.122>
- [36] Rangan BV (2014) Geopolymer concrete for environmental protection. *Indian Concr J* 88:41–59
- [37] Singh P, Sharma K, Hasija V et al (2019) Systematic review on applicability of magnetic iron oxides–integrated photocatalysts for degradation of organic pollutants in water. *Mater Today Chem* 14:100186. <https://doi.org/10.1016/j.mtchem.2019.08.005>
- [38] Brillas E, Garcia-Segura S (2020) Benchmarking recent advances and innovative technology approaches of Fenton, photo-Fenton, electro-Fenton, and related processes: a review on the relevance of phenol as model molecule. *Sep Purif Technol* 237:116337. <https://doi.org/10.1016/j.seppur.2019.116337>
- [39] Wang J, Bai Z (2017) Fe-based catalysts for heterogeneous catalytic ozonation of emerging contaminants in water and wastewater. *Chem Eng J* 312:79–98. <https://doi.org/10.1016/j.cej.2016.11.118>
- [40] Das B, Mohanty K (2019) A review on advances in sustainable energy production through various catalytic processes by using catalysts derived from waste red mud. *Renew Energy* 143:1791–1811. <https://doi.org/10.1016/j.renene.2019.05.114>
- [41] Van Jaarsveld JGS, Van Deventer JSJ (1999) Effect of the alkali metal activator on the properties of fly ash-based geopolymers. *Ind Eng Chem Res* 38:3932–3941. <https://doi.org/10.1021/ie980804b>
- [42] Ken PW, Ramli M, Cheah CB (2015) An overview on the influence of various factors on the properties of geopolymer concrete derived from industrial by-products. *Constr Build Mater* 77:370–395. <https://doi.org/10.1016/j.conbuildmat.2014.12.065>
- [43] Xin L, Xu JY, Li W, Bai E (2014) Effect of alkali-activator types on the dynamic compressive deformation behavior of geopolymer concrete. *Mater Lett* 124:310–312. <https://doi.org/10.1016/j.matlet.2014.03.102>
- [44] Ryu GS, Lee YB, Koh KT, Chung YS (2013) The mechanical properties of fly ash-based geopolymer concrete with alkaline activators. *Constr Build Mater* 47:409–418. <https://doi.org/10.1016/j.conbuildmat.2013.05.069>
- [45] Panagiotopoulou C, Kontori E, Perraki T, Kakali G (2007) Dissolution of aluminosilicate minerals and by-products in alkaline media. *J Mater Sci* 42:2967–2973. <https://doi.org/10.1007/s10853-006-0531-8>
- [46] Chindaprasart P, Jaturapitakkul C, Chalee W, Rattanasak U (2009) Comparative study on the characteristics of fly ash and bottom ash geopolymers. *Waste Manag* 29:539–543. <https://doi.org/10.1016/j.wasman.2008.06.023>
- [47] Davidovits J, Davidovics M, Davidovits N (1994) Process for obtaining a geopolymericalumino-silicate and products thus obtained. 9
- [48] Zhang HY, Kodur V, Wu B et al (2018) Effect of temperature on bond characteristics of geopolymer concrete. *Constr Build Mater* 163:277–285. <https://doi.org/10.1016/j.conbuildmat.2017.12.043>
- [49] Adak D, Sarkar M, Maiti M et al (2015) Anti-microbial efficiency of nano silver-silica modified geopolymer mortar for eco-friendly green construction technology. *RSC Adv* 5:64037–64045. <https://doi.org/10.1039/c5ra12776a>
- [50] Aliabdo AA, Abd Elmoaty AEM, Salem HA (2016) Effect of cement addition, solution resting time and curing characteristics on fly ash based geopolymer concrete performance. *Constr Build Mater* 123:581–593. <https://doi.org/10.1016/j.conbuildmat.2016.07.043>
- [51] Nurrudin MF, Haruna S, Mohammed BSM, Sha'aban IG (2018) Methods of curing geopolymer concrete: a review. *Int J Adv Appl Sci* 5:31–36. <https://doi.org/10.21833/ijaas.2018.01.005>
- [52] Mo BH, Zhu H, Cui XM et al (2014) Effect of curing temperature on geopolymerization of metakaolin-based

- geopolymers. *Appl Clay Sci* 99:144–148. <https://doi.org/10.1016/j.clay.2014.06.024>
- [53] Giasuddin HM, Sanjayan JG, Ranjith PG (2013) Strength of geopolymer cured in saline water in ambient conditions. *Fuel* 107:34–39. <https://doi.org/10.1016/j.fuel.2013.01.035>
- [54] Wang Y, Liu X, Zhang W et al (2020) Effects of Si/Al ratio on the efflorescence and properties of fly ash based geopolymer. *J Clean Prod* 244:118852. <https://doi.org/10.1016/j.jclepro.2019.118852>
- [55] Yao X, Yang T, Zhang Z (2016) Compressive strength development and shrinkage of alkali-activated fly ash–slag blends associated with efflorescence. *Mater Struct Constr* 49:2907–2918. <https://doi.org/10.1617/s11527-015-0694-3>
- [56] Allahverdi A, Najafi Kani E, Hossain KMA, Lachemi M (2015) *Methods to control efflorescence in alkali-activated cement-based materials*. Woodhead Publishing Limited, Cambridge
- [57] Vafaei M, Allahverdi A (2017) High strength geopolymer binder based on waste-glass powder. *Adv Powder Technol* 28:215–222. <https://doi.org/10.1016/j.apt.2016.09.034>
- [58] Xue X, Liu YL, Dai JG et al (2018) Inhibiting efflorescence formation on fly ash–based geopolymer via silane surface modification. *Cem Concr Compos* 94:43–52. <https://doi.org/10.1016/j.cemconcomp.2018.08.013>
- [59] Zhang Z, Yao X, Zhu H (2010) Potential application of geopolymers as protection coatings for marine concrete II. microstructure and anticorrosion mechanism. *Appl Clay Sci* 49:7–12. <https://doi.org/10.1016/j.clay.2010.04.024>
- [60] Glasby T, Day J, Genrich R, Aldred J (2015) EFC geopolymer concrete aircraft pavements at Brisbane West Wellcamp Airport, vol 11, pp 1–9
- [61] Davis G, Montes C, Eklund S (2017) Preparation of lunar regolith based geopolymer cement under heat and vacuum. *Adv Space Res* 59:1872–1885. <https://doi.org/10.1016/j.asr.2017.01.024>
- [62] Anu Karthi AKS, Cindrella L (2019) Self-humidifying novel chitosan-geopolymer hybrid membrane for fuel cell applications. *Carbohydr Polym* 223:115073. <https://doi.org/10.1016/j.carbpol.2019.115073>
- [63] Davidovits J, France S (2017) Recent progresses in concretes for nuclear waste and uranium waste containment. *J Nat Gas Sci Eng* 38:323–332
- [64] Salehi S, Khattak MJ, Bwala AH, Karbalaie FS (2017) Characterization, morphology and shear bond strength analysis of geopolymers: implications for oil and gas well cementing applications. *J Nat Gas Sci Eng* 38:323–332. <https://doi.org/10.1016/j.jngse.2016.12.042>
- [65] Davidovits J (2002) 30 Years of successes and failures in geopolymer applications. market trends and potential breakthroughs. In: *Geopolymer 2002 conference*, pp 1–16. <https://doi.org/10.1017/CBO9781107415324.004>
- [66] Lach M, Korniejenko K, Mikula J (2016) Thermal insulation and thermally resistant materials made of geopolymer foams. *Procedia Eng* 151:410–416. <https://doi.org/10.1016/j.proeng.2016.07.350>
- [67] Kim HK, Lee HK (2010) Acoustic absorption modeling of porous concrete considering the gradation and shape of aggregates and void ratio. *J Sound Vib* 329:866–879. <https://doi.org/10.1016/j.jsv.2009.10.013>
- [68] Liew YM, Heah CY, Yuan LL et al (2017) Formation of one-part-mixing geopolymers and geopolymer ceramics from geopolymer powder. *Constr Build Mater* 156:9–18. <https://doi.org/10.1016/j.conbuildmat.2017.08.110>
- [69] Bai C, Colombo P (2018) Processing, properties and applications of highly porous geopolymers: a review. *Ceram Int* 44:16103–16118. <https://doi.org/10.1016/j.ceramint.2018.05.219>
- [70] Jämstrop E, Strømme M, Bredenberg S (2012) Influence of drug distribution and solubility on release from geopolymer pellets—a finite element method study. *J Pharm Sci* 101:1803–1810. <https://doi.org/10.1002/jps>
- [71] Chen H, Zhang YJ, He PY et al (2020) Coupling of self-supporting geopolymer membrane with intercepted Cr(III) for dye wastewater treatment by hybrid photocatalysis and membrane separation. *Appl Surf Sci* 515:146024. <https://doi.org/10.1016/j.apsusc.2020.146024>
- [72] Falah M, MacKenzie KJD, Knibbe R et al (2016) New composites of nanoparticle Cu(I) oxide and titania in a novel inorganic polymer (geopolymer) matrix for destruction of dyes and hazardous organic pollutants. *J Hazard Mater* 318:772–782. <https://doi.org/10.1016/j.jhazmat.2016.06.016>
- [73] Ge Y, Yuan Y, Wang K et al (2015) Preparation of geopolymer-based inorganic membrane for removing Ni²⁺ from wastewater. *J Hazard Mater* 299:711–718. <https://doi.org/10.1016/j.jhazmat.2015.08.006>
- [74] Chen S, Zhang W, Sorge LP, Seo D (2019) Exploratory synthesis of low-silica nanozeolites through geopolymer chemistry. *Cryst Growth Des* 19:1167–1171. <https://doi.org/10.1021/acs.cgd.8b01636>
- [75] Chen L, Zheng K, Liu Y (2017) Geopolymer-supported photocatalytic TiO₂ film: preparation and characterization. *Constr Build Mater* 151:63–70. <https://doi.org/10.1016/j.conbuildmat.2017.06.097>
- [76] Al-Zeer MIM, Mackenzie KJD (2019) Fly ash-based geopolymers as sustainable bifunctional heterogeneous catalysts and their reactivity in friedel-crafts acylation reactions. *Catalysts*. <https://doi.org/10.3390/catal9040372>

- [77] Song Y, Li Z, Zhang J et al (2020) A low-cost biomimetic heterostructured multilayer membrane with geopolymer microparticles for broad-spectrum water purification. *ACS Appl Mater Interfaces*. <https://doi.org/10.1021/acsami.0c00440>
- [78] Zhang YJ, He PY, Yang MY, Kang L (2017) A new graphene bottom ash geopolymeric composite for photocatalytic H₂ production and degradation of dyeing wastewater. *Int J Hydrog Energy* 42:20589–20598. <https://doi.org/10.1016/j.ijhydene.2017.06.156>
- [79] He P, Wang M, Fu S et al (2016) Effects of Si/Al ratio on the structure and properties of metakaolin based geopolymer. *Ceram Int* 42:14416–14422. <https://doi.org/10.1016/j.ceramint.2016.06.033>
- [80] Tavor D, Wolfson A, Shamaev A, Shvarzman A (2007) Recycling of industrial wastewater by its immobilization in geopolymer cement. *Ind Eng Chem Res* 46:6801–6805. <https://doi.org/10.1021/ie0616996>
- [81] Catauro M, Bollino F, Papale F, Lamanna G (2014) Investigation of the sample preparation and curing treatment effects on mechanical properties and bioactivity of silica rich metakaolin geopolymer. *Mater Sci Eng C* 36:20–24. <https://doi.org/10.1016/j.msec.2013.11.026>
- [82] Tian Q, Nakama S, Sasaki K (2019) Immobilization of cesium in fly ash-silica fume based geopolymers with different Si/Al molar ratios. *Sci Total Environ* 687:1127–1137. <https://doi.org/10.1016/j.scitotenv.2019.06.095>
- [83] Novais RM, Pullar RC, Labrincha JA (2020) Geopolymer foams: an overview of recent advancements. *Prog Mater Sci*. <https://doi.org/10.1016/j.pmatsci.2019.100621>
- [84] Tan TH, Mo KH, Ling TC, Lai SH (2020) Current development of geopolymer as alternative adsorbent for heavy metal removal. *Environ Technol Innov* 18:100684. <https://doi.org/10.1016/j.eti.2020.100684>
- [85] Asim N, Alghoul M, Mohammad M et al (2019) Emerging sustainable solutions for depollution: geopolymers. *Constr Build Mater* 199:540–548. <https://doi.org/10.1016/j.conbuildmat.2018.12.043>
- [86] da Costa Rocha AC, Scaratti G, Moura-nickel CD et al (2020) Economical and technological aspects of copper removal from water using a geopolymer and natural zeolite. *Water Air Soil Pollut* 361:1–15
- [87] Papa E, Medri V, Paillard C et al (2019) Geopolymer-hydroxalite composites for CO₂ capture. *J Clean Prod* 237:117738. <https://doi.org/10.1016/j.jclepro.2019.117738>
- [88] Saufi H, El Alouani M, Alehyen S et al (2020) Photocatalytic degradation of methylene blue from aqueous medium onto perlite-based geopolymer. *Int J Chem Eng*. <https://doi.org/10.1155/2020/9498349>
- [89] Siyal AA, Shamsuddin MR, Rabat NE et al (2019) Fly ash based geopolymer for the adsorption of anionic surfactant from aqueous solution. *J Clean Prod* 229:232–243. <https://doi.org/10.1016/j.jclepro.2019.04.384>
- [90] Waijarean N, Mackenzie KJD, Asavapisit S et al (2017) Synthesis and properties of geopolymers based on water treatment residue and their immobilization of some heavy metals. *J Mater Sci* 52:7345–7359. <https://doi.org/10.1007/s10853-017-0970-4>
- [91] Chen H, Zhang YJ, He PY et al (2020) Novel activated carbon route to low-cost geopolymer based porous composite with high mechanical resistance and enhanced CO₂ capacity. *Microporous Mesoporous Mater*. <https://doi.org/10.1016/j.micromeso.2020.110282>
- [92] Minelli M, Papa E, Medri V et al (2018) Characterization of novel geopolymer-zeolite composites as solid adsorbents for CO₂ capture. *Chem Eng J* 341:505–515. <https://doi.org/10.1016/j.ccej.2018.02.050>
- [93] Minelli M, Medri V, Papa E et al (2016) Geopolymers as solid adsorbent for CO₂ capture. *Chem Eng Sci* 148:267–274. <https://doi.org/10.1016/j.ces.2016.04.013>
- [94] Sazali N (2020) Review A review of the application of carbon-based membranes to hydrogen separation. *J Mater Sci* 55:11052–11070. <https://doi.org/10.1007/s10853-020-04829-7>
- [95] Liu X, Wu Y, Li M et al (2020) Effects of graphene oxide on microstructure and mechanical properties of graphene oxide-geopolymer composites. *Constr Build Mater* 247:118544. <https://doi.org/10.1016/j.conbuildmat.2020.118544>
- [96] Hausmann A, Duke MC, Demmer T (2012) Membrane processing: dairy and beverage applications. In: *Membrane processing*, pp 17–51
- [97] Khanzada NK, Farid MU, Kharraz JA et al (2020) Removal of organic micropollutants using advanced membrane-based water and wastewater treatment: a review. *J Membr Sci* 598:117672. <https://doi.org/10.1016/j.memsci.2019.117672>
- [98] Zhang G, Jin W, Xu N (2018) Design and fabrication of ceramic catalytic membrane reactors for green chemical engineering applications. *Engineering* 4:848–860. <https://doi.org/10.1016/j.eng.2017.05.001>
- [99] Fard AK, McKay G, Buekenhoudt A et al (2018) Inorganic membranes: preparation and application for water treatment and desalination. *Materials (Basel)*. <https://doi.org/10.3390/ma11010074>
- [100] Oliveira SSL, Oliveira SSL, da Silva Barbosa Ferreira R et al (2019) Development of hollow fiber membranes with alumina and waste of quartzite. *Mater Res* 22:1–7. <https://doi.org/10.1590/1980-5373-MR-2019-0171>

- [101] Lee A, Elam JW, Darling SB (2016) Membrane materials for water purification: design, development, and application. *Environ Sci Water Res Technol* 2:17–42. <https://doi.org/10.1039/c5ew00159e>
- [102] Tang S, Zhang Z, Liu J, Zhang X (2017) Double-win effects of in situ ozonation on improved filterability of mixed liquor and ceramic UF membrane fouling mitigation in wastewater treatment? *J Membr Sci* 533:112–120. <http://doi.org/10.1016/j.memsci.2017.03.035>
- [103] Shao N, Tang S, Li S et al (2020) Defective anal-cime/geopolymer composite membrane derived from fly ash for ultrafast and highly efficient filtration of organic pollutants. *J Hazard Mater* 388:121736. <https://doi.org/10.1016/j.jhazmat.2019.121736>
- [104] Zhu B, Duke M, Dumée LF et al (2018) Short review on porous metal membranes—fabrication, commercial products, and applications. *Membranes (Basel)*. <https://doi.org/10.3390/membranes8030083>
- [105] Mallicoat S, Sarin P, Kriven WM (2005) Novel, alkali-bonded, ceramic filtration membranes. *Ceram Eng Sci Proc* 29:37–45
- [106] Jedidi I, Sai S, Khmakem S et al (2009) New ceramic microfiltration membranes from mineral coal fly ash. *Arab J Chem* 2:31–39. <https://doi.org/10.1016/j.arabjc.2009.07.006>
- [107] Kazemimoghadam M (2010) New nanopore zeolite membranes for water treatment. *Desalination* 251:176–180. <https://doi.org/10.1016/j.desal.2009.11.036>
- [108] Fang J, Qin G, Wei W, Zhao X (2011) Preparation and characterization of tubular supported ceramic microfiltration membranes from fly ash. *Sep Purif Technol* 80:585–591. <https://doi.org/10.1016/j.seppur.2011.06.014>
- [109] Fang J, Qin G, Wei W et al (2013) Elaboration of new ceramic membrane from spherical fly ash for micro filtration of rigid particle suspension and oil-in-water emulsion. *Desalination* 311:113–126. <https://doi.org/10.1016/j.desal.2012.11.008>
- [110] He Y, Cui X, Liu X et al (2013) Preparation of self-supporting NaA zeolite membranes using geopolymers. *J Membr Sci* 447:66–72. <https://doi.org/10.1016/j.memsci.2013.07.027>
- [111] Landi E, Medri V, Papa E et al (2013) Alkali-bonded ceramics with hierarchical tailored porosity. *Appl Clay Sci* 73:56–64. <https://doi.org/10.1016/j.clay.2012.09.027>
- [112] Jing L, Yan H, Yuan Y et al (2014) The preparation and characterization of geopolymer based inorganic membranes. *Key Eng Mater* 602–603:80–83. <https://doi.org/10.4028/www.scientific.net/KEM.602-603.80>
- [113] Zhang J, He Y, Wang YP et al (2014) Synthesis of a self-supporting faujasite zeolite membrane using geopolymer gel for separation of alcohol/water mixture. *Mater Lett* 116:167–170. <https://doi.org/10.1016/j.matlet.2013.11.008>
- [114] Singh G, Bulasara VK (2015) Preparation of low-cost microfiltration membranes from fly ash. *Desalin Water Treat* 3994:1–9. <https://doi.org/10.1080/19443994.2013.855677>
- [115] Xu M, He Y, Wang C et al (2015) Preparation and characterization of a self-supporting inorganic membrane based on metakaolin-based geopolymers. *Appl Clay Sci* 115:254–259. <https://doi.org/10.1016/j.clay.2015.03.019>
- [116] Azarshab M, Mohammadi F, Maghsoodloorad H, Mohammadi T (2016) Ceramic membrane synthesis based on alkali activated blast furnace slag for separation of water from ethanol. *Ceram Int* 42:15568–15574. <https://doi.org/10.1016/j.ceramint.2016.07.005>
- [117] Chen M, Zhu L, Dong Y et al (2016) Waste-to-resource strategy to fabricate highly porous whisker-structured mullite ceramic membrane for simulated oil-in-water emulsion wastewater treatment. *ACS Sustain Chem Eng* 4:2098–2106. <https://doi.org/10.1021/acssuschemeng.5b01519>
- [118] Suresh K, Pugazhenth G, Uppaluri R (2016) Fly ash based ceramic microfiltration membranes for oil–water emulsion treatment: parametric optimization using response surface methodology. *J Water Process Eng* 13:27–43. <https://doi.org/10.1016/j.jwpe.2016.07.008>
- [119] Wei Z, Hou J, Zhu Z (2016) High-aluminum fly ash recycling for fabrication of cost-effective ceramic membrane supports. *J Alloys Compd* 683:474–480. <https://doi.org/10.1016/j.jallcom.2016.05.088>
- [120] Bai C, Colombo P (2017) High-porosity geopolymer membrane supports by peroxide route with the addition of egg white as surfactant. *Ceram Int* 43:2267–2273. <https://doi.org/10.1016/j.ceramint.2016.10.205>
- [121] Li Q, He Y, Xu M et al (2017) Study on the removal of Ca^{2+} and Mg^{2+} in water by the geopolymer-based inorganic membrane. *Chongqing Funct Mater* 48:1215–1220. <https://doi.org/10.3969/j.issn.1001-9731.2017.01.039>
- [122] Mohammadi F, Mohammadi T (2017) Optimal conditions of porous ceramic membrane synthesis based on alkali activated blast furnace slag using Taguchi method. *Ceram Int* 43:14369–14379. <https://doi.org/10.1016/j.ceramint.2017.07.197>
- [123] Xu M, He Y, Wang Y, Cui X (2017) Preparation of a non-hydrothermal NaA zeolite membrane and defect elimination by vacuum-inhalation repair method. *Chem Eng Sci* 158:117–123. <https://doi.org/10.1016/j.ces.2016.10.001>
- [124] Naveed A, Saeed F, Khraisheh M et al (2019) Porosity control of self-supported geopolymeric membrane through

- hydrogen peroxide and starch additives. *Desalin Water Treat* 152:11–15. <https://doi.org/10.5004/dwt.2019.23895>
- [125] Naveed A, Noor-ul-Amin KM et al (2019) Desalination and water treatment synthesis and characterization of fly ash based geopolymeric membrane for produced water treatment synthesis and characterization of fly ash based geopolymeric membrane for produced water treatment. *Desalin Water Treat* 161:126–131. <https://doi.org/10.5004/dwt.2019.24283>
- [126] Wang J, Ge Y, He Y et al (2019) A porous gradient geopolymer-based tube membrane with high PM removal rate for air pollution. *J Clean Prod* 217:335–343. <https://doi.org/10.1016/j.jclepro.2019.01.268>
- [127] Xu M, He Y, Liu Z et al (2019) Preparation of geopolymer inorganic membrane and purification of pulp-papermaking green liquor. *Appl Clay Sci* 168:269–275. <https://doi.org/10.1016/j.clay.2018.11.024>
- [128] Zhang YJ, Chen H, He PY, Juan Li C (2019) Developing silica fume-based self-supported ECR-I zeolite membrane for seawater desalination. *Mater Lett* 236:538–541. <https://doi.org/10.1016/j.matlet.2018.10.167>
- [129] Goswami KP, Pugazhenth G (2020) Treatment of poultry slaughterhouse wastewater using tubular micro filtration membrane with fly ash as key precursor. *J Water Process Eng* 37:101361. <https://doi.org/10.1016/j.jwpe.2020.101361>
- [130] He PY, Zhang YJ, Chen H et al (2020) Low-cost and facile synthesis of geopolymer-zeolite composite membrane for chromium(VI) separation from aqueous solution. *J Hazard Mater* 392:122359. <https://doi.org/10.1016/j.jhazmat.2020.122359>
- [131] Li CJ, Zhang YJ, Chen H, He PY (2020) High value-added utilization of silica fume to synthesize ZSM-35 zeolite membrane for Cd²⁺ removal. *Mater Lett* 260:126940. <https://doi.org/10.1016/j.matlet.2019.126940>
- [132] Li L, Shi Q, Huang L et al (2020) Green synthesis of faujasite-La_{0.6}Sr_{0.4}Co_{0.2}Fe_{0.8}O_{3-δ} mineral nanocomposite membrane for low temperature advanced fuel cells. *Int J Hydrogen Energy*. <https://doi.org/10.1016/j.ijhydene.2020.05.275>
- [133] Luukkonen T, Yliniemi J, Sreenivasan H et al (2020) Ag- or Cu-modified geopolymer filters for water treatment manufactured by 3D printing, direct foaming, or granulation. *Sci Rep* 10:1–14. <https://doi.org/10.1038/s41598-020-64228-5>
- [134] Subaer S, Haris A, Irhamsyah A et al (2020) Pervaporation membrane based on laterite zeolite-geopolymer for ethanol-water separation. *J Clean Prod* 249:119413. <https://doi.org/10.1016/j.jclepro.2019.119413>
- [135] Vieira L, Maschio LJ, De Araújo EP et al (2019) Development of geopolymers for catalyst support applications. *Mater Res*. <https://doi.org/10.1590/1980-5373-MR-2018-0770>
- [136] Gupta P, Paul S (2014) Solid acids: green alternatives for acid catalysis. *Catal Today* 236:153–170. <https://doi.org/10.1016/j.cattod.2014.04.010>
- [137] SCOPUS (2020) Research with the words catalytic AND geopolymer. https://www.scopus.com/results/results.uri?numberOffields=0&src=s&clickedLink=&edit=&editSaveSearch=&origin=searchbasic&authorTab=&affiliationTab=&advancedTab=&scint=1&menu=search&tablin=&searchterm1=catalytic+AND+geopolymer&field1=TITLE_ABS_KEY&dateType=. Accessed 15 April 2020
- [138] Černý Z, Jakubec I, Bezdička P, Štengl V (2009) Preparation of photocatalytic layers based on geopolymer. *Ceram Eng Sci Proc* 29:113–122
- [139] Ancora R, Borsa M, Cassar L (2010) Titanium dioxide based photocatalytic composites and derived products on a metakaolin support, vol 1, pp 1–5
- [140] Sazama P, Bortnovsky O, Dědeček J et al (2011) Geopolymer based catalysts-new group of catalytic materials. *Catal Today* 164:92–99. <https://doi.org/10.1016/j.cattod.2010.09.008>
- [141] Gasca-Tirado JR, Manzano-Ramírez A, Villaseñor-Mora C et al (2012) Incorporation of photoactive TiO₂ in an aluminosilicate inorganic polymer by ion exchange. *Microporous Mesoporous Mater* 153:282–287. <https://doi.org/10.1016/j.micromeso.2011.11.026>
- [142] Zhang YJ, Liu LC, Xu Y et al (2012) A new alkali-activated steel slag-based cementitious material for photocatalytic degradation of organic pollutant from waste water. *J Hazard Mater* 209–210:146–150. <https://doi.org/10.1016/j.jhazmat.2012.01.001>
- [143] Zhang Y, Liu L (2013) Fly ash-based geopolymer as a novel photocatalyst for degradation of dye from wastewater. *Particuology* 11:353–358. <https://doi.org/10.1016/j.partic.2012.10.007>
- [144] Zhang YJ, Liu LC, Ni LL, Wang BL (2013) A facile and low-cost synthesis of granulated blast furnace slag-based cementitious material coupled with Fe₂O₃ catalyst for treatment of dye wastewater. *Appl Catal B Environ* 138–139:9–16. <https://doi.org/10.1016/j.apcatb.2013.02.025>
- [145] Gasca-Tirado JR, Manzano-Ramírez A, Vazquez-Landaverde PA et al (2014) Ion-exchanged geopolymer for photocatalytic degradation of a volatile organic compound. *Mater Lett* 134:222–224. <https://doi.org/10.1016/j.matlet.2014.07.090>

- [146] Zhang YJ, Chai Q (2014) Alkali-activated blast furnace slag-based nanomaterial as a novel catalyst for synthesis of hydrogen fuel. *Fuel* 115:84–87. <https://doi.org/10.1016/j.fuel.2013.06.051>
- [147] Zhang YJ, Kang L, Si HX, Zhang JF (2014) A novel alkali-activated magnesium slag-based nanocomposite for photocatalytic production of hydrogen. *Integr Ferroelectr* 154:120–127. <https://doi.org/10.1080/10584587.2014.904189>
- [148] Candamano S, Frontera P, Macario A et al (2015) Preparation and characterization of active Ni-supported catalyst for syngas production. *Chem Eng Res Des* 96:78–86. <https://doi.org/10.1016/j.cherd.2015.02.011>
- [149] Falah M, MacKenzie KJD, Hanna JV, Page SJ (2015) Synthesis of new composites of inorganic polymers (geopolymers) with metal oxide nanoparticles and their photodegradation of organic pollutants by Mahroo Falah
- [150] Hashimoto S, MacHino T, Takeda H et al (2015) Antimicrobial activity of geopolymers ion-exchanged with copper ions. *Ceram Int* 41:13788–13792. <https://doi.org/10.1016/j.ceramint.2015.08.061>
- [151] Kang L, Zhang YJ, Wang LL et al (2015) Alkali-activated steel slag-based mesoporous material as a new photocatalyst for degradation of dye from wastewater. *Integr Ferroelectr* 162:8–17. <https://doi.org/10.1080/10584587.2015.1037197>
- [152] Sharma S, Medpelli D, Chen S, Seo DK (2015) Calcium-modified hierarchically porous aluminosilicate geopolymer as a highly efficient regenerable catalyst for biodiesel production. *RSC Adv* 5:65454–65461. <https://doi.org/10.1039/c5ra01823d>
- [153] Zhang YJ, Kang L, Liu LC et al (2015) Synthesis of a novel alkali-activated magnesium slag-based nanostructural composite and its photocatalytic performance. *Appl Surf Sci* 331:399–406. <https://doi.org/10.1016/j.apsusc.2015.01.090>
- [154] Alzeer MIM, MacKenzie KJD, Keyzers RA (2016) Porous aluminosilicate inorganic polymers (geopolymers): a new class of environmentally benign heterogeneous solid acid catalysts. *Appl Catal A Gen* 524:173–181. <https://doi.org/10.1016/j.apcata.2016.06.024>
- [155] Duan P, Yan C, Luo W, Zhou W (2016) Effects of adding nano-TiO₂ on compressive strength, drying shrinkage, carbonation and microstructure of fluidized bed fly ash based geopolymer paste. *Constr Build Mater* 106:115–125. <https://doi.org/10.1016/j.conbuildmat.2015.12.095>
- [156] Kang L, Zhang YJ, Yang MY et al (2016) A novel V-doped CeO₂ loaded alkali-activated steel slag-based nanocomposite for photocatalytic degradation of malachite green. *Integr Ferroelectr* 170:1–9. <https://doi.org/10.1080/10584587.2016.1165572>
- [157] Li C, He Y, Tang Q et al (2016) Study of the preparation of CdS on the surface of geopolymer spheres and photocatalyst performance. *Mater Chem Phys* 178:204–210. <https://doi.org/10.1016/j.matchemphys.2016.05.013>
- [158] Strini A, Roviello G, Ricciotti L et al (2016) TiO₂-based photocatalytic geopolymers for nitric oxide degradation. *Materials (Basel)* 9:1–13. <https://doi.org/10.3390/ma9070513>
- [159] Zhang YJ, Yang MY, Zhang L et al (2016) A new graphene/geopolymer nanocomposite for degradation of dye wastewater. *Integr Ferroelectr* 171:38–45. <https://doi.org/10.1080/10584587.2016.1171178>
- [160] Alzeer MIM, MacKenzie KJD, Keyzers RA (2017) Facile synthesis of new hierarchical aluminosilicate inorganic polymer solid acids and their catalytic performance in alkylation reactions. *Microporous Mesoporous Mater* 241:316–325. <https://doi.org/10.1016/j.micromeso.2016.12.018>
- [161] Armayani M, Pratama MA, Subaer S (2017) The properties of nano silver (Ag)-geopolymer as antibacterial composite for functional surface materials. *MATEC Web Conf.* <https://doi.org/10.1051/mateconf/20179701010>
- [162] Kang L, Zhang YJ, Zhang L, Zhang K (2017) Preparation, characterization and photocatalytic activity of novel CeO₂ loaded porous alkali-activated steel slag-based binding material. *Int J Hydrog Energy* 42:17341–17349. <https://doi.org/10.1016/j.ijhydene.2017.04.035>
- [163] Zhang YJ, Zhang K, Kang L, Zhang L (2017) A new In₂O₃ and NiO co-loaded fly ash-based nanostructural geopolymer for photocatalytic H₂ evolution. *Integr Ferroelectr* 182:1–9. <https://doi.org/10.1080/10584587.2017.1352376>
- [164] Zhang YJ, Zhang L, Kang L et al (2017) A new CaWO₄/alkali-activated blast furnace slag-based cementitious composite for production of hydrogen. *Int J Hydrog Energy* 42:3690–3697. <https://doi.org/10.1016/j.ijhydene.2016.07.173>
- [165] Zhang YJ, Zhang L, Zhang K, Kang L (2017) Synthesis of eco-friendly CaWO₄/CSH nanocomposite and photocatalytic degradation of dyeing pollutant. *Integr Ferroelectr* 181:113–122. <https://doi.org/10.1080/10584587.2017.1352401>
- [166] Alzeer MIM, MacKenzie KJD (2018) Synthesis and catalytic properties of new sustainable aluminosilicate heterogeneous catalysts derived from fly ash. *ACS Sustain Chem Eng* 6:5273–5282. <https://doi.org/10.1021/acssuschemeng.7b04923>
- [167] John S, Hu Z, Zhu M (2018) Synthesis of novel geopolymer supported nano bimetallic catalysts and its application

- for isopropanol dehydrogenation. *Key Eng Mater* 777:190–195. <https://doi.org/10.4028/www.scientific.net/KeyEngMater.777.190>
- [168] Saputra E, Nugraha MW, Helwani Z et al (2018) Synthesis of geopolymer from rice husk ash for biodiesel production of *Calophyllum inophyllum* seed oil. *IOP Conf Ser Mater Sci Eng*. <https://doi.org/10.1088/1757-899X/345/1/012019>
- [169] Sarkar M, Maiti M, Maiti S et al (2018) ZnO–SiO₂ nanohybrid decorated sustainable geopolymer retaining anti-biodeterioration activity with improved durability. *Mater Sci Eng C* 92:663–672. <https://doi.org/10.1016/j.msec.2018.07.005>
- [170] Zhang YJ, He PY, Chen H (2018) A novel CdO/graphene alkali-activated steel slag nanocomposite for photocatalytic degradation of dye wastewater. *Ferroelectrics* 522:1–8. <https://doi.org/10.1080/00150193.2017.1391587>
- [171] Zhang YJ, He PY, Chen H, Liu LC (2018) Green transforming metallurgical residue into alkali-activated silicomanganese slag-based cementitious material as photocatalyst. *Materials (Basel)* 11:1–10. <https://doi.org/10.3390/ma11091773>
- [172] Zhang YJ, He PY, Zhang YX, Chen H (2018) A novel electroconductive graphene/fly ash-based geopolymer composite and its photocatalytic performance. *Chem Eng J* 334:2459–2466. <https://doi.org/10.1016/j.cej.2017.11.171>
- [173] Zhang YJ, Zhang YX, Yang MY (2018) Synthesis of environment-friendly graphene reinforced slag-based nanocomposite and performance of photocatalytic H₂ generation. *Ferroelectrics* 522:36–44. <https://doi.org/10.1080/00150193.2017.1391609>
- [174] Bendoni R, Miccio F, Medri V et al (2019) Geopolymer composites for the catalytic cleaning of tar in biomass-derived gas. *Renew Energy* 131:1107–1116. <https://doi.org/10.1016/j.renene.2018.08.067>
- [175] He PY, Zhang YJ, Chen H, Liu LC (2019) Development of an eco-efficient CaMoO₄/electroconductive geopolymer composite for recycling silicomanganese slag and degradation of dye wastewater. *J Clean Prod* 208:1476–1487. <https://doi.org/10.1016/j.jclepro.2018.10.176>
- [176] Zhang YJ, He PY, Yang MY et al (2019) Renewable conversion of slag to graphene geopolymer for H₂ production and wastewater treatment. *Catal Today*. <https://doi.org/10.1016/j.cattod.2019.02.003>
- [177] Bedon A, Carabba L, Bignozzi MC, Glisenti A (2020) Environmentally friendly La_{0.6}Sr_{0.4}Ga_{0.3}Fe_{0.7}O₃ (LSGF)-functionalized fly-ash geopolymers for pollutants abatement in industrial processes. *Catal Lett* 3:2–7. <https://doi.org/10.1007/s10562-020-03132-z>
- [178] Huang J, Li Z, Zhang J et al (2020) In-situ synchronous carbonation and self-activation of biochar/geopolymer composite membrane: enhanced catalyst for oxidative degradation of tetracycline in water. *Chem Eng J*. <https://doi.org/10.1016/j.cej.2020.125528>
- [179] Maiti M, Sarkar M, Maiti S et al (2020) Modification of geopolymer with size controlled TiO₂ nanoparticle for enhanced durability and catalytic dye degradation under UV light. *J Clean Prod* 255:120183. <https://doi.org/10.1016/j.jclepro.2020.120183>
- [180] Petlitckaia S, Barré Y, Piallat T et al (2020) Functionalized geopolymer foams for cesium removal from liquid nuclear waste. *J Clean Prod*. <https://doi.org/10.1016/j.jclepro.2020.122400>
- [181] Su Q, Yang S, He Y et al (2020) Prepared self-growing supported nickel catalyst by recovering Ni(II) from metal wastewater using geopolymer microspheres. *J Hazard Mater* 389:121919. <https://doi.org/10.1016/j.jhazmat.2019.121919>
- [182] Zhang LW, Kai MF, Chen XH (2020) Si-doped graphene in geopolymer: its interfacial chemical bonding, structure evolution and ultrastrong reinforcing ability. *Cem Concr Compos* 109:103522. <https://doi.org/10.1016/j.cemconcomp.2020.103522>
- [183] Hitam CNC, Jalil AA (2020) A review on exploration of Fe₂O₃ photocatalyst towards degradation of dyes and organic contaminants. *J Environ Manag* 258:110050. <https://doi.org/10.1016/j.jenvman.2019.110050>
- [184] Kumar A, Raizada P, Singh P et al (2019) Perspective and status of polymeric graphitic carbon nitride based Z-scheme photocatalytic systems for sustainable photocatalytic water purification. Elsevier, Amsterdam

Publisher's Note Springer Nature remains neutral with regard to jurisdictional claims in published maps and institutional affiliations.